BHABHA ATOMIC RESEARCH CENTRE JAN-FEB 2023

Newsletter

- Safety-Critical Systems
- Sealed Neutron Generator
- Atomic Vapour Diagnostics
- Photoisomerism

IMPROVED BIOMATERIALS

- Glimpses of ISC - 2023
- Solid State Physics Symposium
- Theme Meeting - Hydrogen Energy Technology

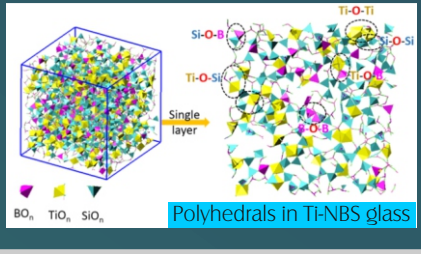

Polyhedrals in Ti-NBS glass


Integrated Test Station

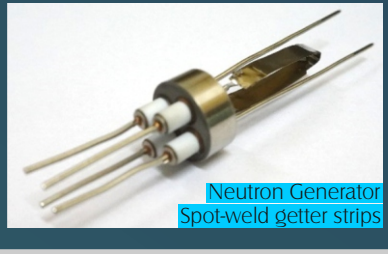
Neutron Generator
Spot-weld getter strips

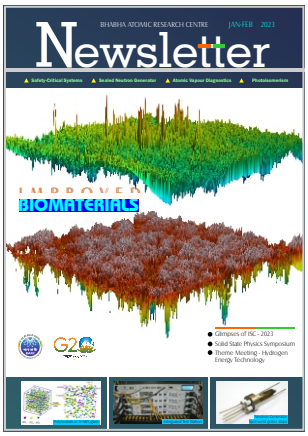

BARC Newsletter
January-February 2023
ISSN: 0976-2108

INTERNATIONAL YEAR OF
MILLETS
2023

EDITOR'S MESSAGE

This issue of BARC Newsletter is a compendium of articles, which encapsulate activities in various domains of basic sciences and engineering, as a part of research and development mandate of the Department of Atomic Energy (DAE). The activities of BARC pertaining to the development of new technologies and materials that contribute to the ongoing efforts for ensuring affordable healthcare, smart and efficient energy systems, neutron generators, pulsed capacitors, which impact positively to the technology landscape, are covered in this issue.

BARC continues a strong impetus for expanding the spectrum of activities in laser based isotope enrichment. It has been pursuing new approaches in process as well as associated diagnostics domain for optimizing the existing laser enrichment processes. Biomaterials find immense applications in curative healthcare industry. It had been demonstrated that the life and bio-efficiency of these materials can be enhanced by coating their surfaces with suitable materials. Corrosion and tribological studies carried out in BARC using zirconia protective coatings on bio alloys have produced a satisfactory outcome and also opened new range of opportunities to the researchers working in this domain. To address the potential issues associated with the leaching of glass material employed in vitrification processes as part of nuclear energy waste management, Molecular Dynamics simulation studies were performed for the first time for ascertaining the efficacy of titanium oxide doped sodium borosilicate glass, which is covered in the form of an article in the issue.

Besides, this issue also reports the in-house development of a sealed D-T neutron generator capable of producing 14.1 MeV high energy neutrons, with practical applications in detection of uranium in bore holes. New outcomes in the domain of Control and Instrumentation are discussed in two articles of this issue.

Globally, water resources management has become a key priority for policymakers in their efforts to ensure holistic and inclusive development. A scholarly work published in the form of a book by a leading expert dealing with scientific aspects of riverine systems and their management, has been covered in this issue in the form of a book review.

We hope this publication would find considerable appeal among the readers. I take this opportunity to thank everyone for their committed efforts that have contributed positively to the preparation and timely release of this issue of newsletter.

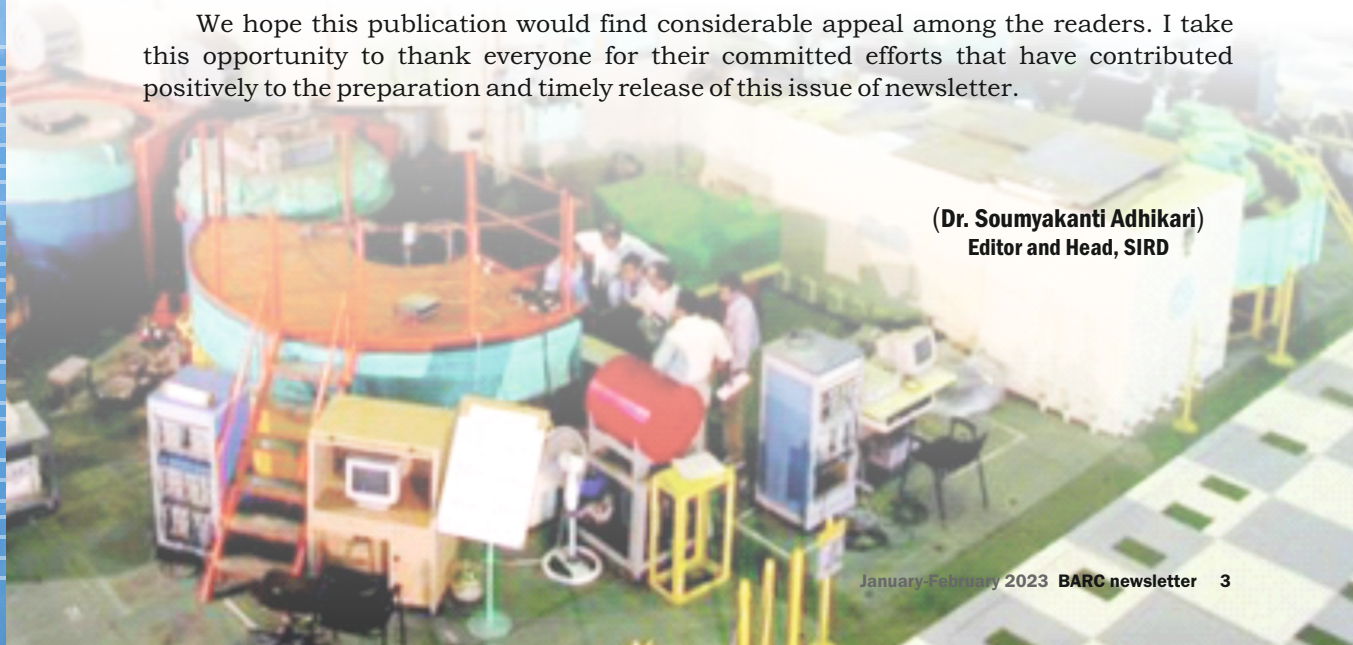

(Dr. Soumyakanti Adhikari)
Editor and Head, SIRD

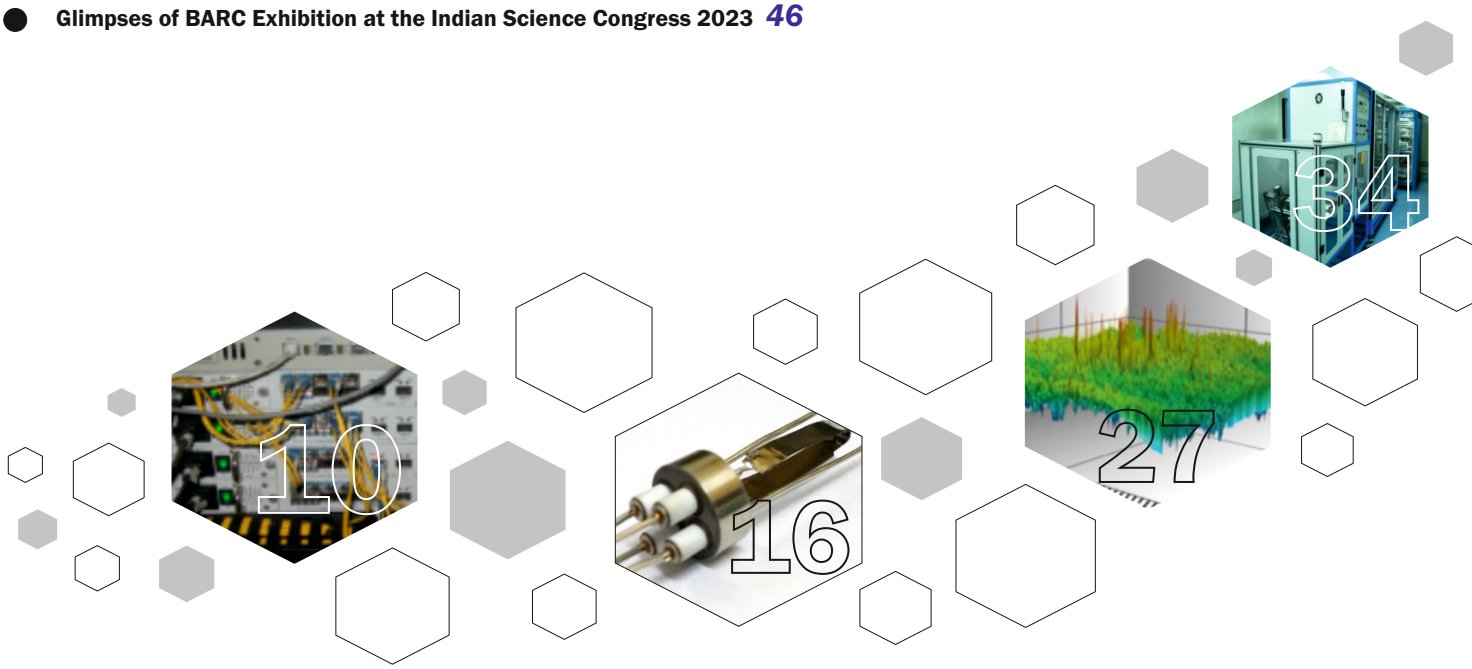

CONTENTS

FORTHCOMING ISSUE

Health Safety & Environment

- Radiation Metrology
- Radiation Dosimetry
- Radiological Surveillance & Monitoring
- Medical Applications
- Emergency Preparedness
- Industrial Hygiene

This page intentionally left blank

C&I Network

1

Indigenous Secure NTP Server for Time Synchronization

Abhishek Borana*, Ashutos Mohanty, Suraj Mukade, D. A. Roy and U. W. Vaidya

Reactor Control Division, Electronics and Instrumentation Group, Bhabha Atomic Research Centre, Mumbai 400085, INDIA

Front View of NTP Server

ABSTRACT

In a distributed network environment, time synchronization across different components is critical for proper chronological sequencing of messages for plant data logging and post-event analysis. In this context, a secure stratum-1 Time-Server module has been indigenously designed and developed for accurate time synchronization across computer-based C&I systems, plant servers and data loggers. It uses GPS time as primary source and provides accurate time synchronization using Network Time Protocol over existing Ethernet network. The indigenous NTP server uses an Operating System (OS)-less design with firmware on Field Programmable Gate Array (FPGA). In this article, we present the design, implementation and deployment scenario of indigenously developed NTP server suitable for use not only in C&I networks, but also in IT infrastructure.

KEYWORDS: *Global Positioning System (GPS), Time Synchronization, Network Time Protocol (NTP), Denial of Service (DoS)*

Introduction

Synchronizing clocks accurately in distributed systems has been an important long-standing challenge. Accurate clocks enable applications to operate on a common time axis across different nodes, which, in turn, enables key functions like consistency, event ordering, causality and scheduling of tasks and resources with precise timing. Time synchronization is of vital importance in variety of applications like distributed data acquisition, event analysis, blackout analysis and stability control of power grid[1], real-time networks based on Time Division Multiple Access(TDMA), financial online trading, large-scale experiments such as particle accelerators[2] etc.

Clock generators and communication channels are not ideal in reality which leads to inaccuracies in time synchronization. In clock generators, quantization, frequency drift due to temperature or ageing, jitter, wander etc. are practically expected. For communication channels, variations in the network delay and variable processing time are problematic and need to be compensated.

Most common protocols governing time transfer are Inter-Range Instrumentation Group (IRIG) time code, Network Time Protocol (NTP) and Precision Time Protocol (PTP). IRIG systems use dedicated coaxial cabling and has disadvantage of added expense and increased time skew. NTP is used to synchronize time across an Internet Protocol (IP) network. In addition to the advantage of accessibility of Ethernet, it also provides synchronization accuracy within 1 to 2 milliseconds which is limited only by network induced jitter. Taking advantage of the existing Ethernet infrastructure allows considerable reuse of in-place hardware and cabling, helping to reduce costs for the physical layer. The PTP has hardware-assisted time stamping, for better accuracy. PTP in ideal conditions with hardware time stamping and transparent clocks can eliminate the effect of the network delay and jitter on the offset measurement and synchronize the system clock with sub-microsecond accuracy. However, NTP is highly resilient. It works with multiple sources, estimates their errors, and selects only good sources for synchronization. In addition, NTP supports authentication with symmetric keys in order to allow clients to verify the authenticity and integrity of received packets and prevent attackers from synchronizing them to a false time.

Commercial NTP Servers have standard software packages running over operating systems like Linux. Unpatched, outdated software along with unused features introduce vulnerabilities making the network prone to concentrated attacks. Keeping in view the concerns and challenges, an indigenous NTP server has been developed in RCnD. Indigenous development will be advantageous from security aspects and will make the design transparent and amenable to verification and validation. The time synchronization functions in the NTP server are implemented on FPGA making it completely OS less. Implementation in FPGA provide accurate time keeping and better network throughput. The device has added features for security like blacklisting or white listing of each client IP. The indigenous design with extensive documentation makes the device amenable to V&V and suitable for deployment in applications having safety and security concerns. In this article, we present the design and implementation of this indigenously developed NTP server which is suitable for use in Control and Instrumentation networks of nuclear power plants and for other general applications.

Network Time Protocol (NTP)

NTP is a networking protocol for clock synchronization between computer systems/embedded systems over packet-switched, variable-latency data networks. NTP provides Coordinated Universal Time (UTC) including scheduled leap second adjustments.

A basic NTP network is composed of a time server and

*Author for Correspondence: Abhishek Borana
E-mail: aborana@barc.gov.in

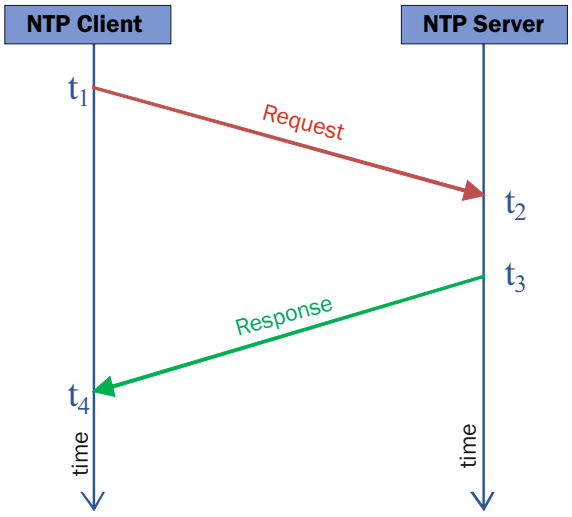

Fig.1: Timing Diagram of NTP client synchronization to a NTP Server.

clients (embedded nodes, workstations etc.). The function of time server is to provide accurate time to the clients. The individual clients run a small program as a background task that periodically queries the server for a precise UTC time reference. These queries are performed at designated time intervals in order to maintain the required synchronization accuracy for the network. In a local network, clients can be synchronized within 1 millisecond.

As depicted in Fig.1, client transmits query packet at time instance t_1. NTP server receives this request at time t_2 and transmits response packet at time t_3. Request and response packet consists of all required time stamps. The client process the response packet and calculate the time offset and the network induced delay as under:

$$\text{Offset} = [(t_2 - t_1) + (t_3 - t_4)] / 2$$

$$\text{Delay} = (t_4 - t_1) - (t_3 - t_2)$$

Client uses intersection algorithm to select accurate time servers and the algorithm is designed to mitigate the effects of variable network latency.

NTP Server is a stand-alone equipment which will maintain accurate time using GPS. Clients will synchronize using NTPv4 (as standardized in RFC5905). A standard NTP server operates in Client/Server, Symmetric Active/Passive or Broadcast modes. However, in our design, NTP server and clients will operate only in Client/Server mode along with client authentication for increased network security. It will also be possible to perform embedded C&I client authentication by server. NTP server is designed and developed such that it will also work with other Windows/Linux based PC nodes having built-in NTP client/server.

The synchronization architecture uses a stratum concept, which is a hierarchical model (tree type) with each server on one level (stratum) serving as a time server to the lower levels. Primary servers are set at the root of the tree as stratum-1 and are synchronized to external clock reference sources such as atomic clocks/GPS/IRNSS (stratum 0). Each of the subsequent levels has a stratum which is one higher than the preceding level as shown in Fig.2. The maximum allowed value for the stratum is 15.

NTP is designed for use by client and server machines with a wide range of capabilities and over a wide range of network delays and jitter characteristics. Commercial equipment and systems use a software package that include

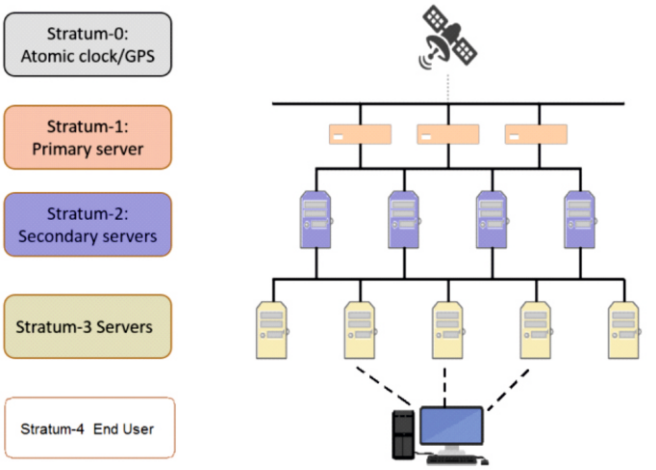

Fig.2: NTP Stratum Model.

Fig.3: Front View of NTP Server.

full suite of NTP options and algorithms, which are relatively complex. The software is ported to a wide variety of platforms ranging from personal computers to supercomputers, its sheer size and complexity is not appropriate for many applications. Server-side software, which do not require clock filtering, selection, clustering or combining algorithm also include a full set of complex software. The design is proprietary in nature, poses security issues and is not amenable to verification and validation. Accordingly, it was useful to explore alternative indigenous strategies using simpler software appropriate for high security applications.

Design

The NTP server, designed and developed as a stand-alone product as shown in Fig.3, works on stratum-1 level as a primary server. It is compatible with NTP clients implemented on commercial operating systems. It also provides configurable relay contact output for interface with existing/legacy C&I systems.

The design consists of NTP Agent implemented using FPGA, GPS receiver with Oven Controlled Crystal Oscillator (OCXO), and a Configuration Agent implemented using microcontroller as shown in Fig.4. The GPS receiver receives GPS signal through antenna. It provides UTC time and a synchronized 10MHz clock to NTP Agent. The NTP Agent (FPGA) is the core element which incorporates concurrent processing for better performance and accurate timing. It acquires time from GPS receiver and uses the synchronized 10MHz clock for time keeping. The FPGA is responsible for time keeping and processing and it acts as the primary NTP server to provide accurate time to various clients.

The NTP agent provides 4 Ethernet interfaces and processes concurrent NTP requests in parallel. It maintains a UTC time and also generates pps signal as a digital output. An internal battery operated RTC is provided to maintain the time till GPS lock is not achieved. For interface with existing plant C&I systems, relay contacts with configurable on-off time and pulse output is provided. Four independent RS485 interfaces are provided over which digital slave clocks can be interfaced using custom protocols.

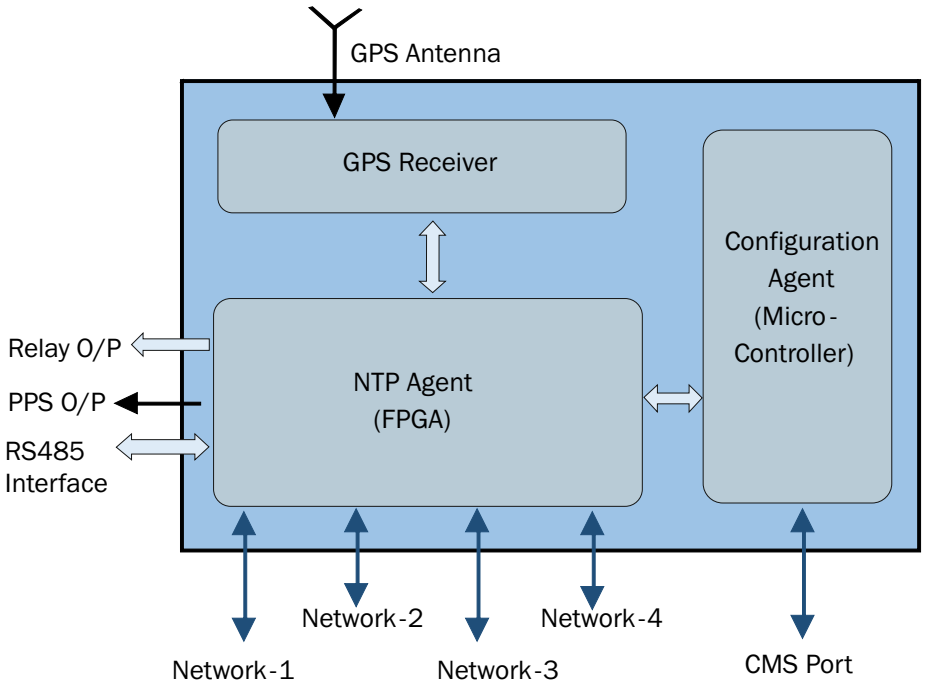

Fig.4: Block Diagram of NTP Server.

The Configuration Agent interfaces with Configuration management software (CMS) for configuration download and transfer of device statistics. It provides a secure web-server interface to a PC through a separate CMS Ethernet port.

Salient Features

The NTP server offers the following general features:

- GPS based Stratum-1 Network Time Protocol Server
- OS less implementation in FPGA
- Four independent NTP engines catering to 4 user ports
- 30,000 NTP requests per second per port
- Oscillator: OCXO ±5ppb
- 1U High 19" Rack mount, Dual Redundant Power Supply
- Power Consumption less than 10 watts
- Qualification: Climatic (Dry Heat and Damp Heat as per IS-9000)

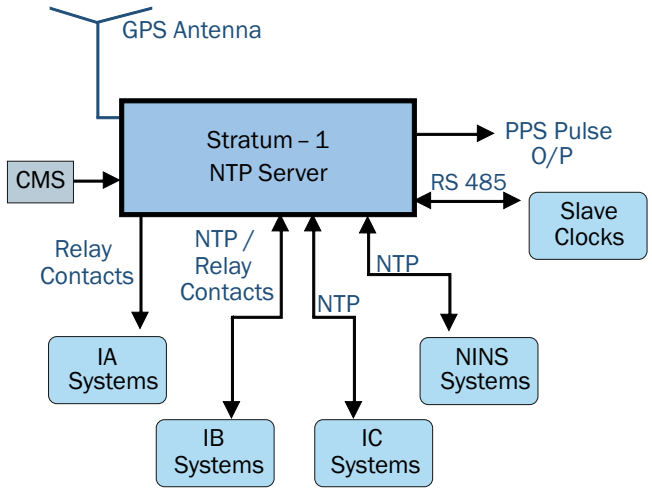

Fig.5: Typical deployment scenario for C&I systems of NPPs.

It offers the following performance features.

- GPS Accuracy: Max ± 35 nsec
- 24 Hour Holdover: Max ±10µsec/day at 25°C (on GPS signal loss)

It provides the following interfaces:

- GPS Interface : TNC
- Network Interface: 4x10/100/1000 Mbps
- Configuration Port : 1x10/100 Mbps
- Relay Output: 32 Contacts
- Digital Output (pps): 2 x Isolated Digital Output
- RS485 for Slave Clock: 4 Nos./10Mbaud

The following security features are incorporated in design:

- One Time programmable NTP stack in FPGA
- OS less NTP stack operation
- Encrypted FPGA configuration
- Whitelisted Clients with specified rate limiting

Security

Millions of hosts use the Network Time Protocol (NTP) to synchronize their computer clocks through timeservers on the Internet. Recently, the security of NTP over internet has come under new scrutiny. NTP plays a major role in UDP amplification attacks[3,4]. Now, there is a new focus on attacks on the NTP protocol itself, both in order to maliciously alter a target's time (*'timeshifting attacks'*) or to prevent a target from synchronizing its clock (*'denial of service' - DoS attacks*)[5]. These attacks are of concern because the correctness of time has a bearing on many other basic protocols and services. For instance, cryptographic protocols use timestamps to prevent replay attacks and limit the use of stale or compromised cryptographic material (e.g., TLS, HSTS, DNSSEC, authentication protocols). Rate limiting of incoming traffic, client authentication and better timing achieved using FPGA

Fig.6: Deployment in ITS lab of RCnD.

implementation makes the indigenous device better in terms of the above mentioned security concerns against the commercially available devices.

Deployment Scenario

Fig.5 depicts a typical deployment scenario of a Master clock System.

The NTP server provides time synchronization services to various C&I systems and time keeping equipment in the plant. Slave clocks provide the interface to the large station clock in control room which is synchronized to the GPS time broadcast by server on a RS485 link. The NTP server unit was designed, fabricated and tested, and it has been installed in Integrated Test Station (ITS) lab of RCnD in BARC. Different C&I systems in the lab were interfaced with the server unit over Ethernet as shown in Fig.6. Subsequently, it was installed and tested for time synchronization in networked seismic stations across Mumbai and Bengaluru. It has also been installed in Dhruva and interfaced to slave clocks in the plant.

Conclusions

Accurate Time synchronization is not only useful in event data logging in a distributed plant environment but is also important in IT infrastructure, distributed sensor network etc. NTP is most common protocol for time synchronization providing accuracy, cost and maintainability benefits over existing Ethernet infrastructure. An indigenous stratum-1 GPS based NTP Server has been designed and developed to provide accurate time synchronization among various C&I systems, plant servers, station clocks, etc. This helps in proper chronological logging of messages for post-event analysis. It is designed to support existing relay-based synchronization of C&I systems and servers. The FPGA based design provides inherent benefit of timing accuracy and stability, and gives an edge over the commercial devices that are equipped with standard software packages and unused features which make the entire network vulnerable to security attacks. Various security features of the device make it suitable for use in plant C&I network and critical IT infrastructure. This device offers an indigenous solution to replace the central clock system in nuclear plants which are expensive and available from limited vendors.

References

[1] Steinhauser, F.; Riesch, C.; Rudigier, M., IEEE 1588 for time synchronization of devices in the electric power industry, Proceedings of the International IEEE Symposium on Precision Clock Synchronization for Measurement, Control and Communication (ISPCS), Portsmouth, NH, USA, 27 September–1 October 2010, 1–6.

[2] Lipinski, M.; Wlostowski, T.; Serrano, J.; Alvarez, P., White rabbit: A PTP application for robust sub-nanosecond synchronization, Proceedings of the 2011 IEEE International Symposium on Precision Clock Synchronization for Measurement, Control and Communication, Munich, Germany, 9–12 September 2011, 25–30.

[3] Czyz, J., Kallitsis, M., Gharaibeh, M., Papadopoulos, C., Bailey, M., Karir, M., Taming the 800 pound gorilla: the rise and decline of NTP distributed denial-of-service (DDoS) attacks, Proceedings of the 2014 Internet Measurement Conference, 2014, 435–448.

[4] Kramer, L., Krupp, J., Makita, D., Nishizoe, T., Koide, T., Yoshioka, K., Rossow, C., AmpPot: monitoring and defending against amplification DDoS attacks, In: Bos, H., Monrose, F., Blanc, G. (eds.) RAID 2015. LNCS, Springer, 2015, 9404, 615–636.

[5] Malhotra, A., Cohen, I.E., Brakke, E., Goldberg, S., Attacking the network time protocol, In: NDSS 2016, February.

Safety-Critical C&I Systems

2

SPERTS: A Tool for Development of Safety-Critical Systems

Suraj Mukade*[1], Pratibha Sawhney[1], Prateek Saxena[1], Ashutosh Kabra[1], Amol Wakankar[1], Ajith K. J.[1], S. T. Sonnis[1], D. A. Roy[1] and Anup Bhattacharjee[2]

[1]*Reactor Control Division, Bhabha Atomic Research Centre, Mumbai 400085, INDIA*
[2]*Security Electronics & Software Systems Division, Bhabha Atomic Research Centre, Mumbai 400085, INDIA*

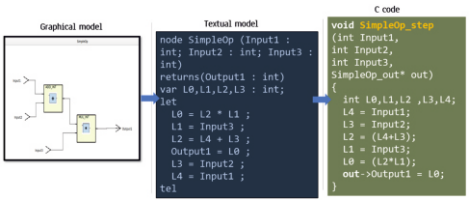

SPERTS Code Generation

ABSTRACT

SPERTS (Safe Programming Environment for Real-Time Systems) is an integrated environment for development of safety-critical systems. Using SPERTS, a developer can build a formal model of the system by specifying the user/system requirements using a higher level graphical language suitable for safety-critical system. The SPERTS language supports function blocks and state-machine constructs with rigorous semantics. A model built using SPERTS i) can be formally verified, ii) helps generate code, which is correct-by-construction and finally iii) produces a deployable code using target specific library. This article presents the SPERTS environment focusing on the enabling techniques behind application development, verification of requirements, validation of the safety properties and automated code generation including test cases.

KEYWORDS: *Safety-critical systems, SPERTS (Safe Programming Environment for Real-Time Systems), Nuclear power plants (NPPs), Building blocks, Model builder*

Introduction

Safe Programming Environment for Real-Time Systems (SPERTS) is a tool, which is developed to design, implement, and verify control systems for safety-critical applications. This tool has been developed at Reactor Control Division, BARC. What makes SPERTS different from conventional programming environment supporting graphical language is its formal (mathematical) model-based development approach.

The key features of the tool include the following.

I) An integrated development environment, which provides a) a graphical modelling tool, b) a code generator, and c) a simulation facility allowing developers to quickly design and verify control systems.

ii) The code generated by SPERTS is designed to be highly reliable, making it suitable for safety-critical applications. This is because of a) the formal model with mathematically defined precise semantics that is built out of the application program (user specifications) and b) the code is generated automatically from the requirements (user specifications as formal model), which is *correct-by-construction*.

iii) It provides tools for verifying the correctness of control systems along with the tools for testing, debugging, formal verification and static analysis. These tools are used to ensure that control systems meet the required safety standards and operate as intended.

iv) SPERTS enforces adherence to Programming Guidelines (PG) by a qualified code generator and built-in logical constructs that are safe to use in safety critical applications.

v) It ensures deterministic response time due to synchronous data flow constructs in the language[1].

*Author for Correspondence: Suraj Mukade
E-mail: suraj@barc.gov.in

The additional features of SPERTS that make this tool unique are automatic test-cases and report generation following standard design template.

Thus, SPERTS in not only an import substitute for highly expensive tools like SCADE [2], but it comes with enhanced features.

The Genesis

SPERTS is designed to provide a programming environment for Diverse Modular Safety Platform (DMSP), which is a computer based configurable platform consisting of a set of dedicated and qualified hardware and software components for use in safety applications of nuclear power plants (NPPs). Using SPERTS, this platform is configured and programmed with system specific application software to build different safety-critical systems.

To this end, SPERTS is built to run on open-source LINUX platform to generate code for safety applications. SPERTS has in-built support for integrating qualified hardware modules such as Input and Output boards through their board interface libraries, thus enabling singleclick hardware-software integration.

Application Development

SPERTS facilitates development for safety-critical applications by following the *V*−model of software development life-cycle (SDLC) conforming to IEC 60880 as shown in Fig.1.

The phases for detailed software design, coding, module integration and testing are integrated into the automated processes supported by SPERTS. All these features help in making the design, development, testing, integration and qualification of applications/systems (developed on DMSP) easier and faster by virtue of its trustworthiness by design.

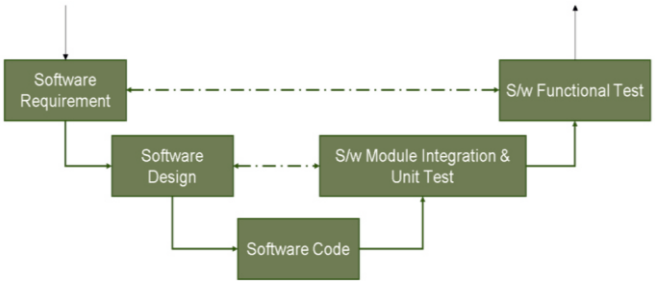

Fig.1: V-Model of SDLC.

Building Blocks of SPERTS

The essential modules that constitute SPERTS to provide an environment for building safety-critical applications using DMSP hardware are discussed briefly in this section. The structural relationship of the SPERTS modules, which help realize the goal of using formal methods of software development through high level user specification is presented in Fig.2. In addition, conformance with the standard development practices[3] is also ensured by design.

Model Builder (MB)

It is a GUI based environment that facilitate building a formal model for application logic using graphical artefacts as well as textual specifications.

It provides seamless integration of state machine and data-flow equations[4] to carry out the model development of software-based control systems and allows hierarchical model of the system i.e., development of system model by composing the models of its sub-components.

Each component of the model is denoted as a node. It is possible to reuse existing nodes of the model for specifying the other higher level nodes. SPERTS supports hierarchical state machines, which allows the designers to easily develop complicated applications in a modular fashion.

The Configuration Module (CM) in the Model Builder facilitates application specific configuration, which allows user to add the required hardware modules, specify the fail-safe state of each input/output, network parameter for communication modules, cycle time of the system etc.

Code Generator (CG)

The first step in automatic code generation involves production of textual representation of the graphical model of the application program. The textual model, generated by Model Builder, is then fed to the syntax and semantic checker module (SSC-CG) of CG, which checks the syntactic and semantic correctness of the textual model. This is followed by generation of an intermediate representation of the textual model in the form of an Abstract Syntax Tree (AST). Subsequently, it generates a target independent C program from the AST, which is semantically equivalent to the functional behaviour of the textual model[5,6]. The code generation process is shown in Fig.3. This generated code is compiled along with required dependencies (such as BSP, OS, system libraries etc.) to produce an executable for deployment on the target safety system.

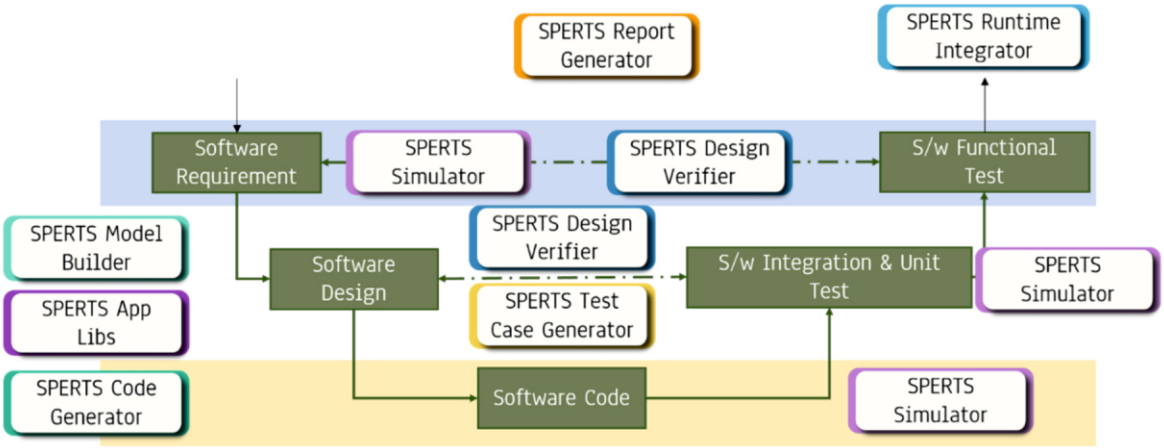

Fig.2: Use of SPERTS modules in SDLC.

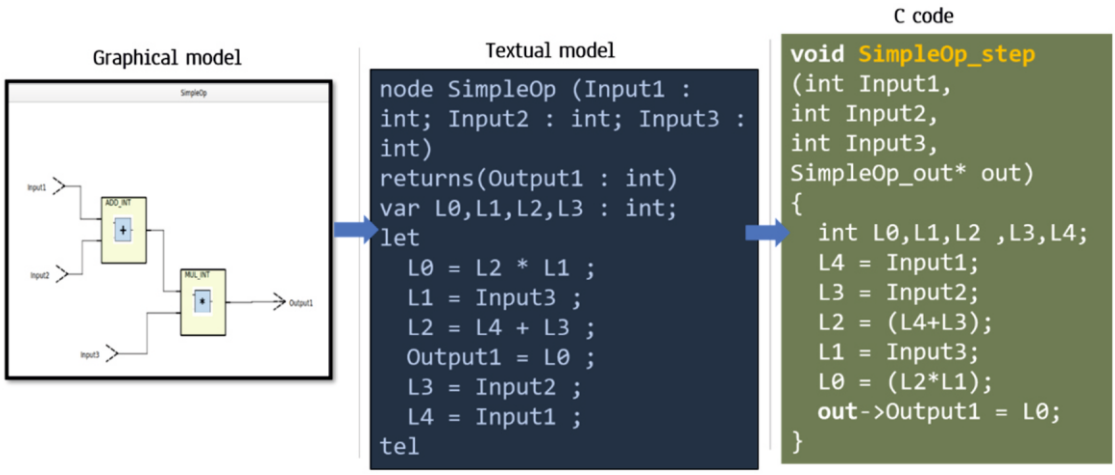

Fig.3: SPERTS Code Generation.

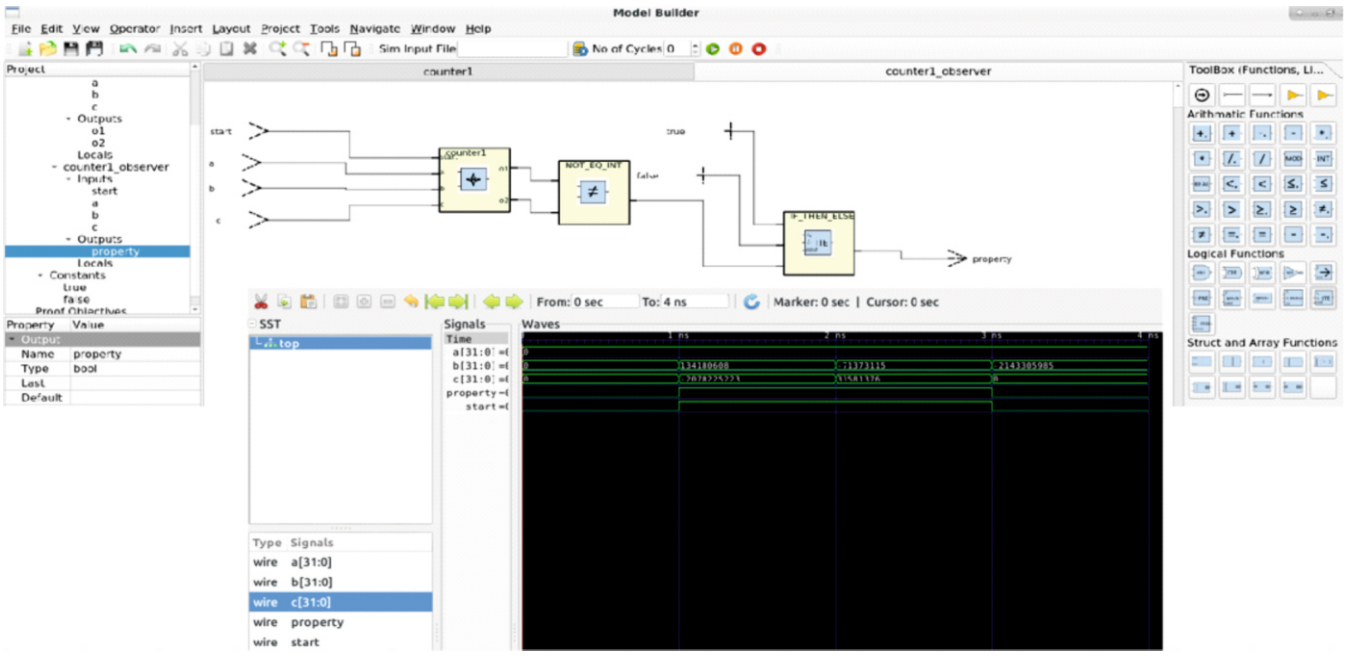

Fig.4: SPERTS Design Verifier.

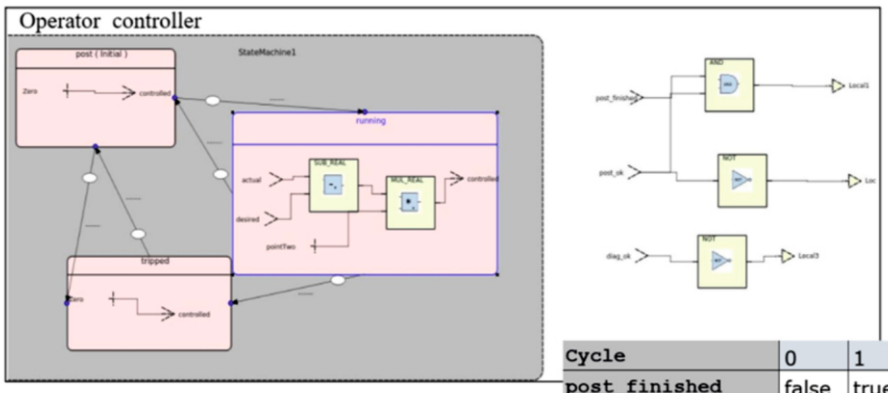

Cycle	0	1	2	3	4	5	6
post_finished	false	true	true	true	true	true	false
post_ok	true	true	true	true	true	true	false
reset	false	false	false	true	false	false	true
diag_ok	true	false	true	true	false	true	false
actual	10.0	10.0	10.0	10.0	10.0	10.0	10.0
desired	5.0	5.0	5.0	5.0	5.0	5.0	5.0
Branches Covered	¬T1, ¬T2	T1	¬T3, ¬T4	T1, T3	T4	¬T5	T2,T5

Fig.5: Test case generation module of SPERTS.

Code generation for Simulation

Simulation is essential to validate the user developed model against any run-time logical error that may manifest. CG module can also be configured to facilitate generation of instrumented C code to support simulation. The instrumented C code exposes the internal state of the application at run-time which enables debugging and validation.

Model Simulator (MS)

This module supports validation of the model by simulation. Model Simulator (MS) enables debugging and simulation of models by executing the instrumented C code. CG module can be configured to generate instrumented C code for both on-host and on-target simulation. The instrumented C code makes the internal state of the application observable by outputting inputs, outputs and internal variables of each node of the application. The CG module for simulation also generates the wrapper function main for compilation and generation of executable. During the execution of the instrumented C code, the observable information is provided to the MS in a format agreed between CG and MS. MS module then graphically displays the state of the application at every instance of execution.

Design Verifier (DV)

This module of SPERTS provides support for Formal Verification using Model Checking technique. A Model Checker is a tool which takes the program and the desired property as inputs and exhaustively searches for possible violations of the property. Note that model checking is fully automatic and requires no human interaction. The main advantage of this technique is that in case the program violates the property; it is reported as the sequence of inputs which led to the violation. This is called as the counterexample, which is an execution trace leading to a state where the property is violated. By

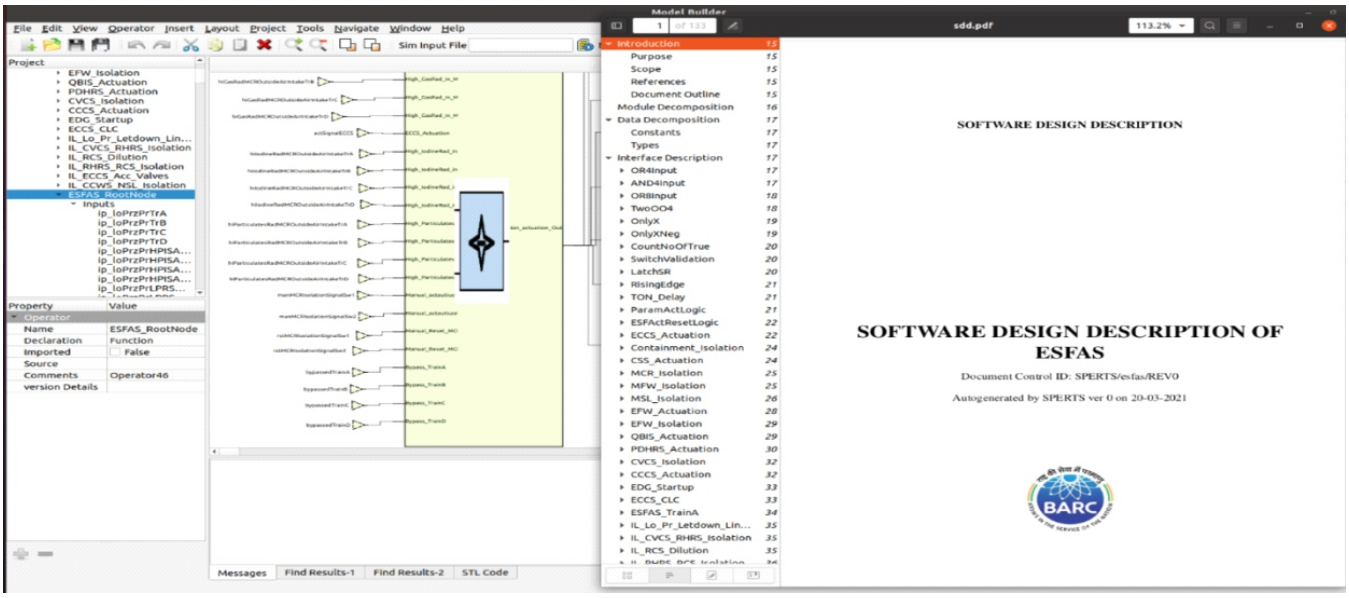

Fig.6: Report Generation Module of SPERTS.

analysing the counterexample, the source(s) of error in the model can be found. By ensuring that the model satisfies safety properties, we increase our confidence in the correctness of the model. The interface of Design Verifier with SPERT MB is presented in Fig.4.

Qualified Application Library (QAL)

This module provides the commonly used set of operators as pre-developed libraries for faster development of application. The qualified group of library operators that are supported by SPERTS QAL are i) logical operators, ii) arithmetic operators, iii) selection and look-up table, iii) trigonometric operator, iv) timer and counting operators, v) triggers, vi) bitwise operators, vii) PID operator, and viii) alarm processing operators.

Automatic Test Case Generator (ATG)

This module facilitates automatic generation of test cases for structural coverage criteria such as branch coverage and statement coverage. The generated test suite can be executed to determine and report the percentage of coverage achieved with respect to the specified coverage criteria. The generated test-cases are encoded as simulation scenarios which are accepted by the Model Simulator module. This scheme is shown in Fig.5.

Report Generator (RG)

Automatic report generation is a useful feature of SPERTS, which takes SPERTS model as input and generates a report describing the design of the application under development. The Report Generator (RG) creates the design documentation in a customized format to the comply with recommended design template as shown in Fig.6. The report is generated as PDF or HTML document.

Conclusions

SPERTS, the integrated development environment for safety-critical applications is presented in this article. The advantages of mixed mode programming using qualified graphical function blocks as well as state machine are also explained. The automated code generation, which guarantees to satisfy the specified safety properties makes this tool most suitable for Diverse Modular Safety Platform in developing safety applications. Furthermore, automated test-case generation facility makes this tool unique among the available ones.

Acknowledgements

The authors thank U. W. Vaidya, Head RCnD, S. Mukhopadhyay, Director, E&IG, BARC and P. R. Patil, former Head RCnD, for extending their support in this endeavour. The authors also thank G. Karmakar for providing technical support in writing the article.

References

[1] N. Halbwachs, P. Caspi, P. Raymond and D. Pilaud, The synchronous data flow programming language LUSTRE, Proceedings of the IEEE, Sept., 1991, 79(9), 1305-1320. doi: 10.1109/5.97300.

[2] Ansys SCADE Suite: Model-Based Development Environment for Critical Embedded Software. https: //www.ansys.com/en-in/products/ embedded-software/ansys-scade-suite.

[3] IEC 60880:2006, Nuclear Power Plants Instrumentation and Control Systems Important to Safety - Software Aspects for Computer-Based Systems Performing Category A Functions, 2006.

[4] A. Benveniste, T. Bourkey, B. Caillaud and M. Pouzet, A hybrid synchronous language with hierarchical automata: Static typing and translation to synchronous code. In Proceedings of the Ninth ACM International Conference on Embedded Software (EMSOFT), Taipei, Taiwan, 2011, 137-148. doi: 10.1145/2038642.2038664.

[5] Dariusz Biernacki, Jean-Louis Colac¸o, Gr´egoire Hamon, and Marc Pouzet, Clock directed modular code generation for synchronous data-flow languages, Proceedings of the 2008 ACM SIGPLAN-SIGBED conference on Languages, compilers, and tools for embedded systems, 2008, 121–130.

[6] Auger, C., Colaçob, J. L., Hamon, G., & Pouzet, M., A formalization and proof of a modular Lustre compiler, 2012.

Fissile Material Detection

3

Development of Sealed Neutron Generator for Fissile Material Detection

Mayank Shukla*, Prashant Singh, Yogesh Kashyap, Tushar Roy, Shefali Shukla, Baribaddala Ravi, M. R. More and L. M. Pant
Technical Physics Division, Bhabha Atomic Research Centre, Mumbai – 400085, INDIA
S. K. Raut, S. G. Sawant, Ram Avtar Jat and S. C. Parida
Product Development Division, Bhabha Atomic Research Centre, Mumbai – 400085, INDIA
N. K. Prasad and M. G. Bagalkar
Electromagnetic Application and Instrumentation Division, Bhabha Atomic Research Centre, Mumbai – 400085, INDIA
S. M. Yusuf
Physics Group, Bhabha Atomic Research Centre, Mumbai – 400085, INDIA

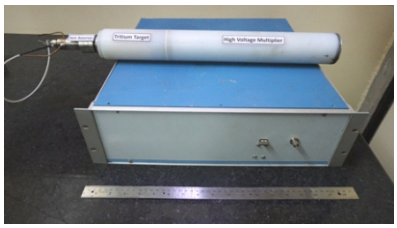

Sealed neutron generator with control electronics inside 19-inch box

ABSTRACT

We present indigenous development of DC accelerator based 14MeV Deuterium(D)-Tritium(T) compact sealed neutron generator for laboratory and field applications. It comprises of a sealed tube with a Penning Ion Source (PIS), metallic D-gas reservoir, beam shaping & accelerating shroud and tritium target holder in-housed in an all metal-to-ceramic joints compact mechanical housing. A micro controlled high current power supply is used to ionize deuterium gas in the ion source. The PIS is operated in pulsed mode with pulse duration ranging from of 100μs to 500μs and up to 1 kHz repletion rate. To produce fusion neutrons, a deuterium ion beam is extracted through an aperture, accelerated to 90kV, and focused on a Tritium target. The ion source and DC acceleration are powered by micro-controlled indigenously built gate pulse generators and high voltage power supply that are controlled by a remote computer using graphical user interface software. The generator gives a neutron yield of ~$8x10^6$ n/s at 80kV with 200μs pulse ON time and 500 Hz repetition rate. It has been used for fissile material detection using prompt fission neutron activation.

KEYWORDS: *Penning ion source, Deuterium, Tritium, Neutron yield, Sealed neutron generator*

Introduction

Compact sealed neutron generators with moderate neutron yield (10^6 to 10^7 n/s) find field applications such mining exploration, oil well logging, coal analysis for power plants etc. These generators, being more handy, also finds use in areas such as detection of special nuclear materials, explosive detection, narcotics detection, material characterization [1-8]. The DC accelerator-based compact sealed generator mainly comprise of an ion source, a D-gas reservoir, acceleration electrode and neutron-producing target. In these generators, a D-D (2.45 MeV) / D-T (14.1 MeV) fusion reaction occurs when an accelerated deuterium ion beam interacts with the target (D or T), producing mono energetic neutrons. The design & development of an indigenous sealed neutron generator is presented in the following sections. Compact micro controlled 3kV high voltage ion source pulsed power supply, 90kV high voltage DC acceleration power supply, constant current (variable upto 8A) gas reservoir heating power supply along with GUI software to control the neutron generator through a remote PC have been designed and developed. In pulsed mode operation with 200μs pulse duration and 500Hz repetition rate, the neutron generator produces 14.1 MeV neutrons with neutron yield ~$8x10^6$ n/s at 80kV acceleration voltage. The generator has been tested for fissile material detection using prompt fission neutron activation. Approximately 3gm and 5gm ^{235}U has been detected in 1000 kg of quartz sand kept in a plastic drum.

*Author for Correspondence: Mayank Shukla
E-mail: mayank@barc.gov.in

Sealed Neutron Generator

As shown in Fig.1, the compact sealed neutron tube is made up of a penning ion source (PIS), a metallic titanium D-gas getter reservoir, a beam shaping and accelerating shroud electrode, and a tritium target holder, which are assembled in a small mechanical assembly with ceramic-to-metal sealing joints. The mechanical assembly is evacuated to ultra-high vacuum (~10^{-8} mbar) through the highly malleable brazed copper tubes. A multi-pin electrical feedthrough provides electrical contacts to anode & cathode of PIS and to gas reservoir metallic getter strips. All metallic joints combining the ion source, high voltage ceramic spacer, shroud electrode and target holder were precision welded under inert gas atmosphere to achieve a leak rate of <10^{-12} mbar litre/s. The neutron tube was detached from the vacuum system using a pinch-off tool.

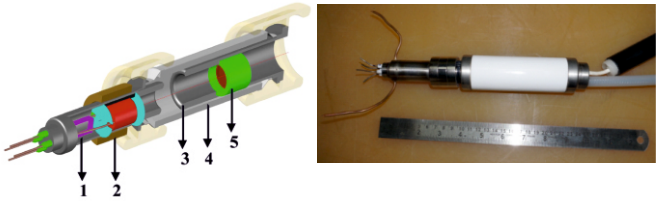

Fig.1: Schematic and assembled sealed neutron tube - 1. Metallic getter strip; 2. PIS; 3. Shroud Electrode; 4. HV Ceramic Spacer and 5. Tritium Target Holder.

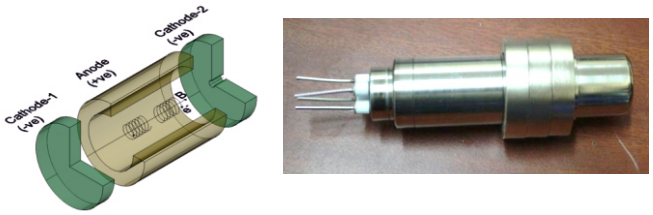

Fig.2: Cold cathode penning Ion Source.

Fig.3: Deuterium loaded metallic titanium getter strips.

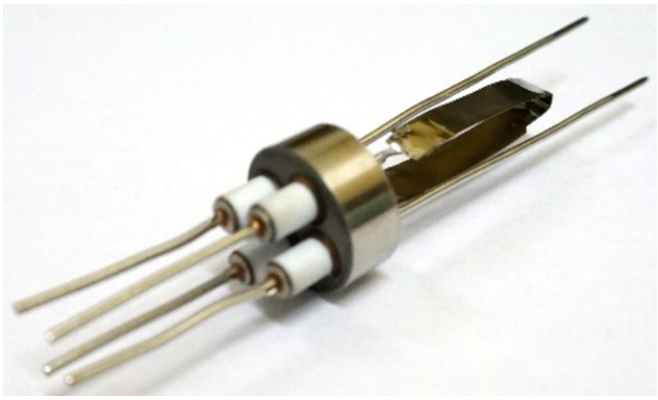

Fig.4: Spot-weld getter strips on feedthrough.

Penning Ion Source

The discharge in the cold cathode Penning ion source is described as a weakly ionized plasma created utilizing DC voltage in a low magnetic field and low gas pressure. A hollow cylindrical anode positioned between two parallel cathode plates in a constant axial magnetic field creates a symmetrical geometry that serves as the penning discharge chamber, as illustrated in Fig.2. A useful ion beam can be retrieved through an aperture in one of the cathode plates. Low sputtering materials in the plasma environment such as high purity titanium for anode and thin tantalum (0.1mm thick) for cathode were chosen for stable operation of the ion source.

Deuterium Gas Reservoir Getter and Neutron Target

Metallic gas reservoir getter is required for controlled release of deuterium gas into the ion source in sealed neutron tube. Titanium metal of Grade-1 in the form of thin strip (40mm x 6mm x 0.1mm thick) was used as gas storage material. Two such strips were evacuated to ultra-high vacuum (UHV) and heated to 500^{0}C activation temperature inside a UHV gas handling manifold. The UHV system consists of reaction vessel, pre-calibrated volumes, pressure and vacuum gauges and turbo molecular pumping station. In order to adsorb a known amount of deuterium gas, activated strips were exposed to the gas at about 200^{0}C. The pressure-volume relationship was used to compute the deuterium content in the titanium while monitoring the system pressure. The final composition of the TiDx phase was calculated to be x~0.7 from the final pressure of the system. This corresponds to ~ 130cc of deuterium gas adsorbed in the two titanium strips. Fig.3 shows the physical appearance of the strips loaded with deuterium. These strips were spot-welded on the feedthrough pins for controlled release of gas in the plasma chamber of the ion source using DC power supply of 6-8A as shown in Fig.4. The assembled ion source with metallic getter (Fig.2) was tested for gas sorption/desorption and discharge inside an all-metallic leak tight UHV system under static vacuum conditions up to pressure of the order of 10^{-2} mbar.

A high purity grade-1 Ti thin film (~3μm) deposited on an OFHC copper disk (16mm diameter and 0.8mm thick) using chemical vapor deposition was used to fabricate tritium neutron target used in the tube [9]. The target was fabricated using a similar UHV gas manifold as described above with glove box. Tritium loading in the Ti film was carried after activating the film up to 500^{0}C under high vacuum [10]. An ~3 Ci (±10%) tritium target on copper disk was fixed on the target holder electrode as shown in Fig.1.

High Voltage Power Supplies and Control Electronics

As illustrated in Fig.5, the sealed neutron tube requires following power supplies for operation: a 3kV pulsed power supply for ion source, a 100kV high voltage DC acceleration power supply, and a constant current (varying up to 8A) getter heating power supply. The compact ion source (3kV/20mA) and DC acceleration (100kV/2mA) power supplies were designed and developed using inverter followed by rectifier/multiplier to achieve the required voltages. The block diagram of the inverter is shown in Fig.6. Ion source power supply was used to bias a MOSFET based gate pulse generator for pulsed operation of 200μs pulse duration and 500Hz repetition rate.

A Cockcroft-Walton high voltage multiplier allows for high voltage DC acceleration up to -100kV. The shroud electrode

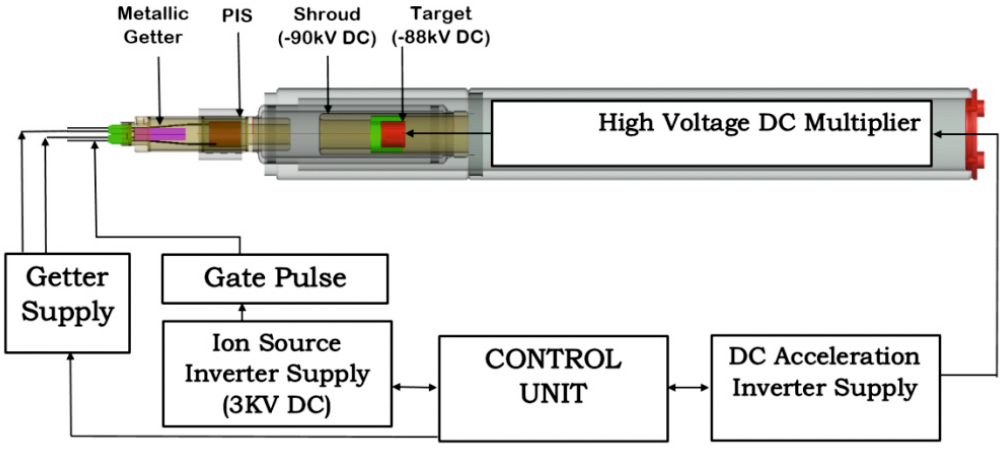

Fig.5: Block diagram of Neutron Generator.

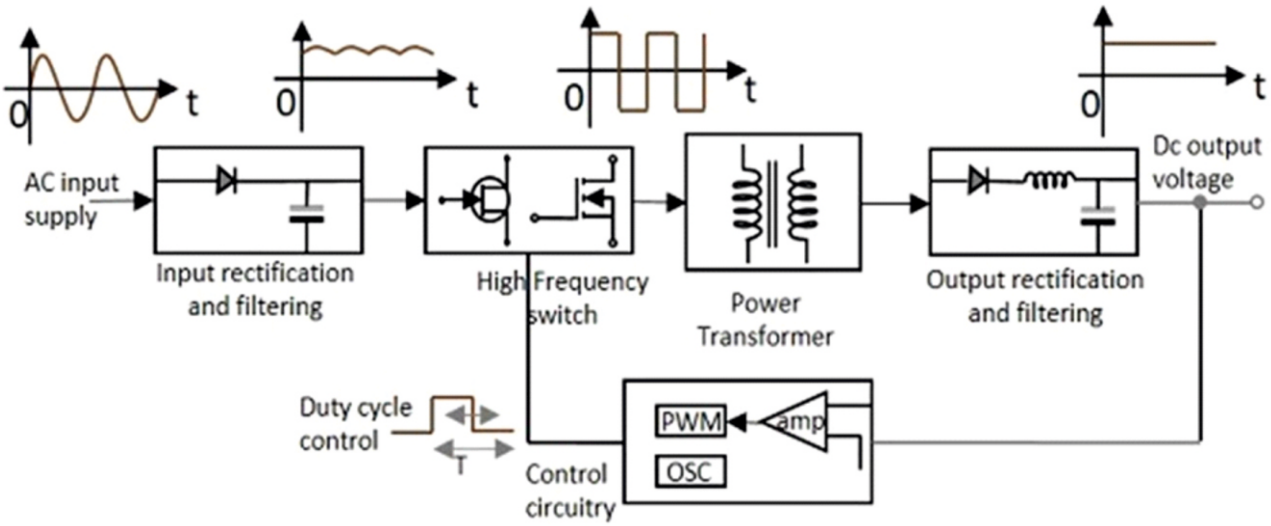

Fig.6: Inverter block diagram.

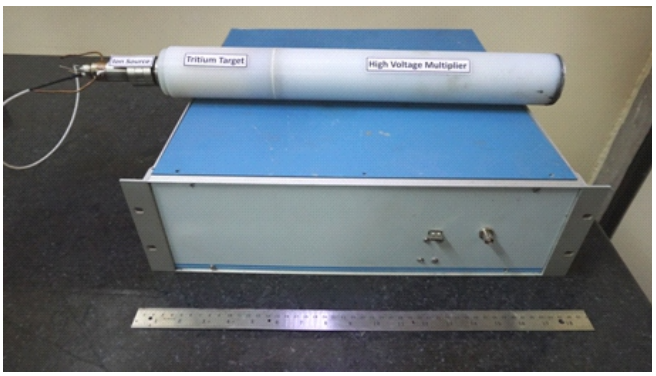

Fig.7: Sealed neutron generator with control electronics inside 19-inch box.

biased slightly positive with respect to the target electrode voltage between the shroud electrode and the target electrode prevents secondary electron back current from entering the ion source, ensuring steady neutron tube operation. The high voltage multiplier in combination with set of reversed biased Zener diodes generates -88KV DC for shroud electrode and -90KV DC for target. This multiplier section is insulated inside a cylindrical nylon assembly filled with high voltage insulation oil that also serves as coolant for the neutron target. The entire electronics along with the microcontroller -based control circuits have been incorporated in a 19-inch box. The neutron source along with the electronic control box is shown in Fig.7. GUI software to control the neutron generator through a remote PC has also been developed as shown in Fig.8.

Testing of Neutron Generator

Sealed neutron generator was tested using the indigenously developed electronics. For pulsed operation, PIS have been biased up to ~3KV voltage and pulse duration

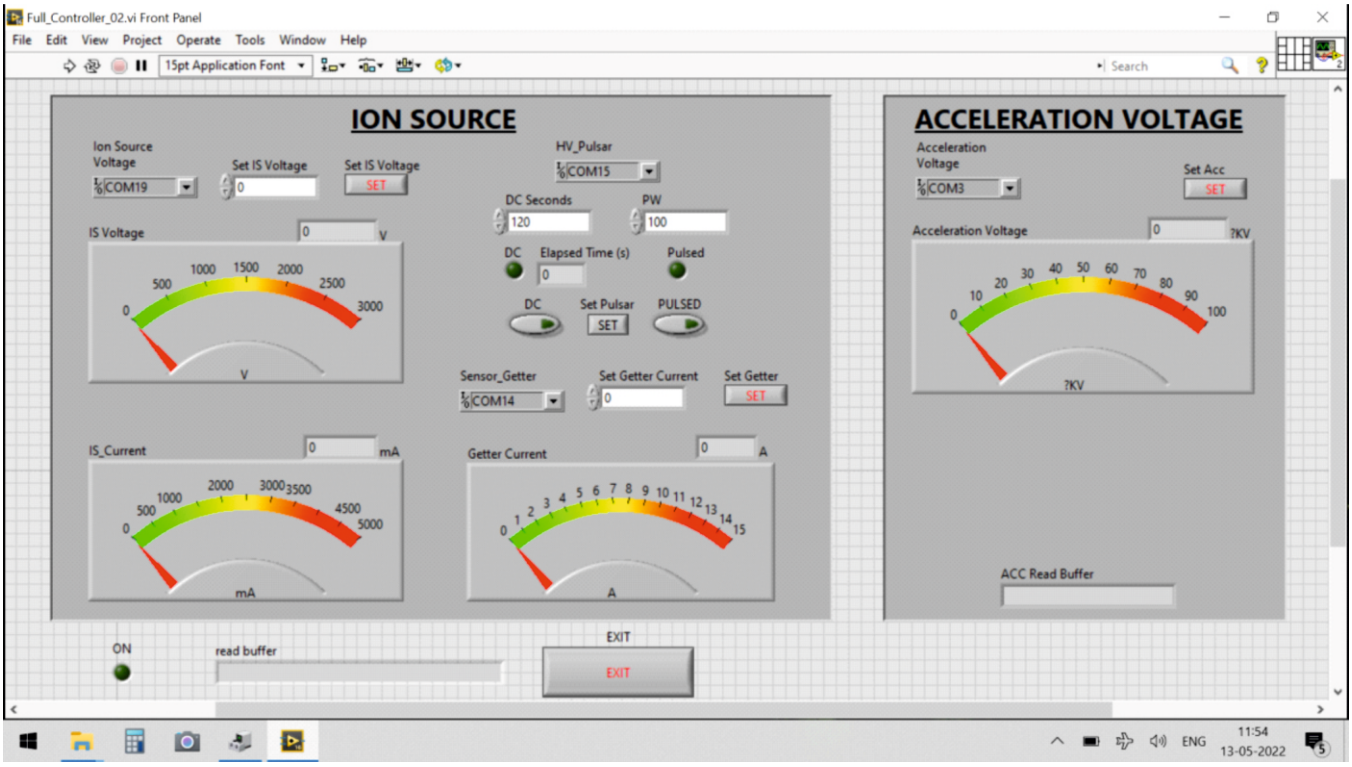

Fig.8: GUI control of sealed neutron generator.

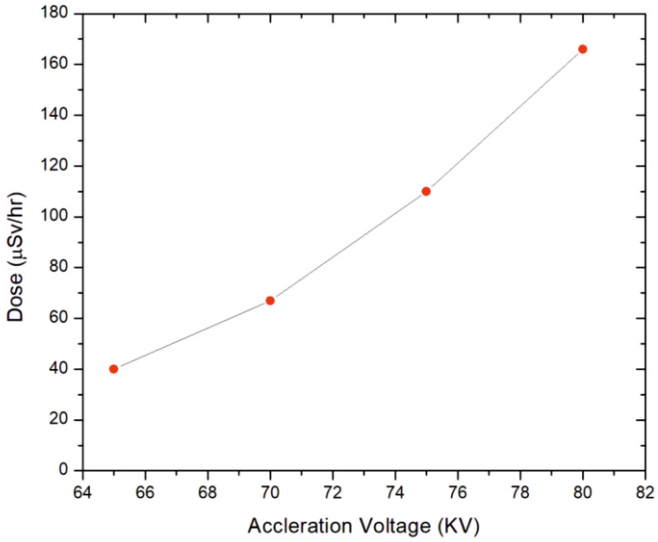

Fig.9: Measured neutron dose vs acceleration Voltage.

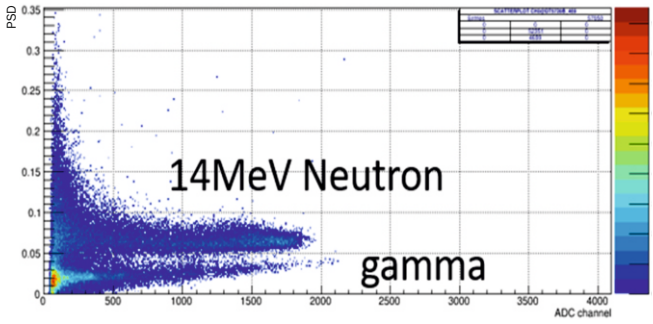

Fig.10: Neutron Energy measurement using liquid scintillator detector.

~200µs with a repletion rate of 500Hz. The high voltage DC acceleration has been varied up to 80kV. The measured neutron dose as a function of acceleration voltage for typical operation is shown in Fig.9. Neutron yield ~8x10^6 n/s was estimated by counting number of bubbles using bubble detector, detector sensitivity and dose equivalent for D-T (14.1MeV) neutrons [11]. Fig.10 & Fig.11 show the 2-D PSD measurement of 14.1 MeV neutrons using liquid scintillator detector and neutron spectra recorded using neutron spectrometer, respectively.

Fissile material detection using sealed neutron generator

The indigenously developed sealed neutron generator has been used for the detection of fissile material using prompt fission neutron activation. Approximately 1000kg of quartz sand was filled in a plastic drum of 1meter diameter having centrally located cavities to insert neutron generator and He-3 detector. The neutron generator was operated in repetitive mode with 200µs pulse duration and 500Hz repetition frequency giving a neutron yield of ~8x10^{6}n/s. Fig.12 show the signals recorded for 3gm and 5gm of uranium disk placed in the sand with respect to the background signal from the sand.

Conclusion

Compact DC acceleration based sealed D-T neutron generator producing 14.1 MeV high energy neutrons has been designed and developed indigenously. This generator is useful for both field as well as applications that demand low probing volume and moderate neutron yield (~10^7 n/s). The sub-assemblies of the generator, such as the penning ion source, deuterium gas reservoir, acceleration, and target electrodes,

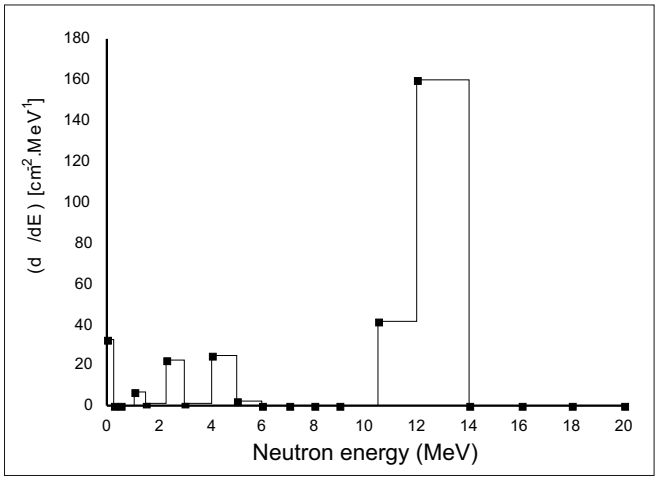

Fig.11: Neutron spectra of D-T generator kept on HDPE block using neutron spectrometer.

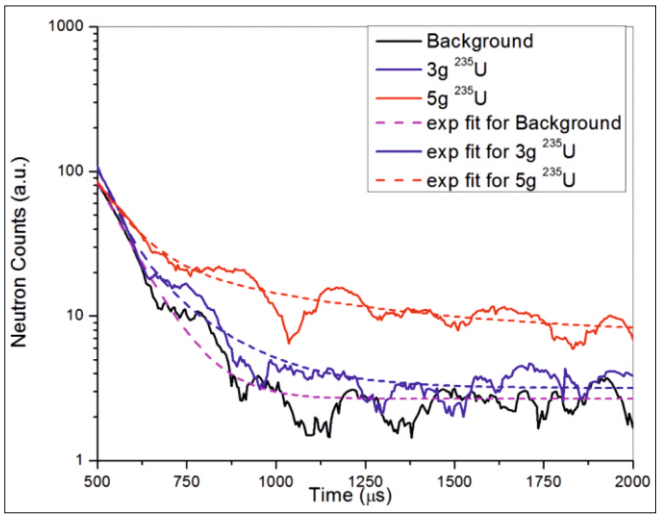

Fig.12: Experimental plots for 3gm and 5gm ^{235}U in 1000kg of quartz sand.

have been designed and developed in-house, precision welded, and pinched off to make a compact sealed neutron tube. Micro controlled high voltage ion source & DC acceleration power supplies, gate pulse generator, gas reservoir heating supply have also been designed and developed indigenously. The generator is being operated by remote computer using graphical user interface software. The generator gave a neutron yield of ~8x10^6 n/s at 80kV with 200µs pulse ON time and 500 Hz repetition rate. This generator has been successfully used for fissile material detection in laboratory using prompt fission neutron activation. It is being modified for making a PFN logging probe for field applications such as detection of uranium in a borehole.

Contributions

The Neutron and Synchrotron Physics Section (N&SRPS), TPD has conceptualized, designed and developed the compact sealed neutron generator that includes penning ion source, high voltage DC acceleration and target electrodes, deuterium gas reservoir, high voltage and other control electronics along with GUI software etc.

Process Development Division has contributed in loading of deuterium gas in Ti metal strips and tritium in Ti film on copper substrate.

Mechanical Fabrication Section, EmA&ID has contributed in fabrication of mechanical components for ion source and high voltage housing and low temperature pulse TIG welding of the metallic joints.

Acknowledgements

Authors are thankful to S. Kannan, Director, RC&I Group, BARC for his support and encouragement. We are also thankful to S. K. Malhotra, Head, EmA&ID, BARC for his continuous support. Special thanks to R. P. Kushwaha and Santosh Kumar, Material Joining Section, Materials Science Division, BARC for precision laser welding of the multi-pin feedthrough of the penning ion source and N. A. Nalawde, EMAS, EmA&ID for EDM wire cutting of feedthrough pins. We acknowledge the support provided by NP&HIAS, NPD and X&NTS, TPD for neutron energy measurement using liquid scintillator detector. RSS, RSSD is also acknowledged for their support in measurement of neutron spectra of the D-T neutron generator.

References

[1] Neutron Generators for Analytical Purposes", IAEA Radiation Technology Reports Series No. 1, 2012.

[2] J. Reijonen, E. O. Lawrence, Compact Neutron Generators for Medical, Home Land, Security and Planetary Exploration, Proc. Particle Accelerator Conference, Knoxville, Tennessee, 2005.

[3] Y. Wu, Development of a Compact Neutron Generator to be Used for Associated Particle Imaging using a RF-Driven Ion Source, Ph.D. thesis, University of California, Berkeley, 2009.

[4] E. S. Grishnyaev, Development of miniature neutron generators for science and well logging, 4th Asian Forum for Accelerators and Detectors (AFAD -2013), February 25-26, 2013, Novosibirsk, Russia.

[5] Alvarez, R. A., Dougan, A. D., Rowland, M. R., Wang T. F., Neutron Interrogation to Identify Chemical Elements with an Ion-Tube Neutron Source, J. Radioanal. Nucl. Chem., 1995, 192, 73–80.

[6] P. C. Womble, F. J. Schultz, G. Vourvopoulos, Non-Destructive Characterization using Pulsed Fast-Thermal Neutrons, Nucl. Instrum. Methods Physics Res.B, 1995, 99, 757–760.

[7] T. Gozani, D. Strellis, Advances in Neutron Based Bulk Explosive Detection, Nucl. Instrum. Methods Physics Res. B, 2007, 261, 1-2, 311-315.

[8] Y. Kashyap, A. Agrawal, T. Roy, P. S. Sarkar, M. Shukla, T. Patel, A. Sinha, Differential Die Away Analysis for detection of 235U in a metallic matrix, Nucl. Instrum. Methods Physics Res. A, 2016, 806B, 1-4.

[9] Mayank Shukla, Niranjan Ramgir, Baribaddala Ravi, Prashant Singh, K. R. Sinju, A. K. Debnath, K. P. Muthe, Yogesh Kashyap, Tushar Roy, Shefali Shukla, Mahendra More, K. G. Bhushan, K. C. Rao , S. G. Sawant , Ram Avtar Jat, S. K. Raut, S. C. Parida, S. C. Gadkari and T.V. Chandrasekhar Rao, Indigenous Development of Neutron Producing Targets for DC Accelerator based Neutron Generators, BARC Internal Report, BARC/2020/I/006.

[10] Mayank Shukla, Niranjan Ramgir, Prashant Singh, Yogesh Kashyap, A. K. Debnath, K. P. Muthe, Tushar Roy, Baribaddala Ravi, Shefali Shukla, S. G. Sawant, S. K. Raut, Ram Avtar Jat, S. C. Parida, K. G. Bhushan and K. C. Rao, Titanium Hydride targets for Portable Neutron Generator applications, 2020, BARC Newsletter, 370.

[11] Impact of Switching to the ICRP-74, Neutron Flux-to-Dose Equivalent Rate Conversion Factors at the Sandia National Laboratory Building 818 Neutron Source Range, Sandia Report, D. C. Ward, Sandia National Laboratories, Albuquerque, N. Mex., USA, SAND 2009, 1144.

Vitrification of Nuclear Wastes

4

Atomistic Design of TiO_2 Doped Sodium Borosilicate Glass

Pooja Sahu[1,2], Sk. Musharaf Ali*[1,2], K. T. Shenoy[1], A. Arvind[3], D. Banerjee[3], Sanjay Kumar[3] and S. Manohar[3]

[1]*Chemical Engineering Division, Bhabha Atomic Research Centre, Mumbai – 400085, INDIA*
[2]*Homi Bhabha National Institute, Anushaktinagar, Mumbai – 400094, INDIA*
[3]*Nuclear Recycle Group, Bhabha Atomic Research Centre, Mumbai – 400085, INDIA*

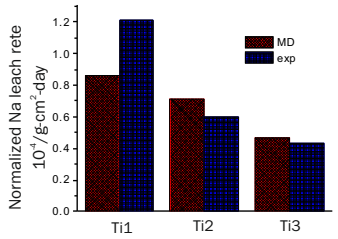

Effect of TiO_2 concentration on Na leach rate.

ABSTRACT

Selection of a suitable doping oxide for incorporation in sodium borosilicate glass for radioactive waste immobilization is one of the key challenges in nuclear waste management. Atomic simulations provide a route for initial screening and thus lessen the time and number of trial experiments. In that perspective, robust molecular dynamics (MD) simulations were carried out to identify the role of TiO_2 in augmenting mechanical, chemical and thermal strength of NBS glass. Computed results were well matched with the experimental findings. The present computational and experimental findings might be useful in the future design of NBS glass for nuclear waste immobilization.

KEYWORDS: *Sodium borosilicate glass, Nuclear waste management, Molecular dynamics, Nuclear waste immobilization*

Introduction

The application of borosilicate glasses in radioactive waste immobilization [1, 2] arises due to a combination of useful material properties including high chemical durability, resistance to crystallization/devitrification and the ability to accommodate a wide diversity of cations within its structure. Basic understanding about the macroscopic properties of the glasses is pursued through microscopic structure at the atomic and molecular level. Considering the numerous applicability, and improved performance of titanium (Ti) added glass and glass ceramics, significant research has been conducted in this direction [3, 4, 5, 6]. Owing to high field strength and polarization ability of titanium ions, TiO_2 doped optical glasses have been profoundly used for optical applications [4, 6]. Besides, TiO_2 is used as a fascinating component in glass jewels and crystal wares. In addition, a decrease in viscosity of glass melts and improved mechanical strength of vitrified glasses can be achieved by increasing the TiO_2 content of the waste form [7]. The lack of understanding about the microscopic structure of these glasses and the local environment around Ti ions is the centre of the problem while dealing with optimization of Ti doped glasses for numerous applications.

Owing to their low solubility, it is difficult to experimentally synthesize the Ti doped silicate glasses. It has been observed that the presence of modifier ions offers the ease possibility of introducing Ti and other rare earth metal ions in the glass network. In absence of modifiers, doping of Ti and other rare earth metal ions can't be reach to high values as they tend to form cluster in these glasses [8, 9].

In spite of technical challenges, the peculiar behaviour of TiO_2 bearing glasses is still not fully understood. A large discrepancy has been noticed about the preferential occurrence of TiO_4, TiO_5 and TiO_6 structural forms in Ti doped glasses [5, 10, 11]. Therefore, a systematic investigation is needed to draw an appropriate conclusion. Very little to nothing has been reported about the effects of TiO_2 on the mechanical and other properties of ternary sodium borosilicate glasses [4, 12, 13].

The present article is devoted to understand the effects associated with the doping of titanium ions in sodium borosilicate glasses using molecular dynamics (MD) simulations. Though the experimental techniques continue to be the major source for finding the structural information and properties of materials, the recent advancement in MD like computational techniques may provide more valuable facts in many circumstances, especially when it is difficult to perform appropriate experiments. MD is extensively used to provide the microscopic insights, which might explain the experimentally observed phenomena.

Computational Protocols

The glass simulations were conducted with LAMMPS package [14]. The interaction between atoms was simulated using the combination of Buckingham potential (for short-range interactions) and Coulomb potential (for long-range interactions), together known as Van Beest, Kramer, Van Santen (BKS) potential model [15].

$$U_{vdw} = \sum_{i=1}^{N}\sum_{j>i}^{N} A_{ij} e^{-r_{ij}/\rho_{ij}} - \frac{C_{ij}}{r_{ij}^6} \quad (1)$$

$$U_{coul} = \frac{q_i q_j}{4\pi\varepsilon r_{ij}} \quad (2)$$

The parameters ρ_{ij}, A_{ij} and C_{ij} control the narrowness of potential model. The separation between the i^{th} and j^{th} atom, having partial charge q_i and q_j respectively is represented by r_{ij} and ε is the permittivity. The forcefield parameters of simulated glasses can be found in our previous papers[16, 17].

Particle-Particle-Particle Mesh (PPPM) method[18] was employed to account for the long-range interactions. The

*Author for Correspondence: Sk. Musharaf Ali
E-mail: musharaf@barc.gov.in

partial charge on the atoms were taken to be composition dependent [19]. All systems were initially heated at 5000 K using the canonical (NVT) ensemble for 10 ns in order to remove the memory effects. This was followed by NVT quenching at a rate of 0.4 K/ps. The systems were furthermore equilibrated for 20 ns dynamics using the isothermal–isobaric ensemble (NPT)[20] at 300 K and P = 1 atm. Further, the production runs were performed for 30 ns, and the generated data was utilized for the analysis of structural and dynamical properties of simulated glass, with methods as discussed in our earlier articles. [16, 17].

Results and Discussion

Titanium dioxide does not form a glass alone, but it can be incorporated in significant amounts into other glass-forming oxide systems. The addition of TiO_2 to glasses contributes to improve glass-forming ability, chemical durability and stabilization of the glass structure. In general, vitrified sodium borosilicate glass for nuclear applications contain TiO_2 concentration less than 1% weight [21]. However, for optical and other applications, the role of TiO_2 with concentration 0-30% in ternary and quaternary borosilicate glasses [11, 22-25] and 0-50% in binary silicate glasses[5, 26, 11] have been studied in the light of experiments and MD simulations. In the present study, the sodium borosilicate (NBS) doped with TiO_2 molar composition varied from 2% to 20% were considered. For all the simulated glasses, the numbers of SiO_2, B_2O_3 and Na_2O molecules were kept constant as 680, 340 and 238 respectively, whereas the number of TiO_2 was varied to be 25, 63, 126, 189, 252, 314 and 378. The percentage contribution of TiO_2 was varied from 1.95%, 4.77%, 9.10%, 13.06%, 16.69% and 19.97%, denoted as Ti1, Ti2, Ti3, Ti4, Ti5, and Ti6 respectively. The corresponding simulated snapshots are shown in Fig. 1.

The computed density was seen to increase with increasing TiO_2 concentration in the glass matrix (Fig.2). The increase in density with increasing Ti concentration was supposed to be related with the higher molecular weight (79.87 g mol^{-1}) of TiO_2 than the other components (SiO_2 = 60.08 g mol^{-1}, B_2O_3 = 69.62 g mol^{-1}, Na_2O = 61.98 g mol^{-1}).

In addition to density, the volume of glass was also increased while increasing TiO_2, as network structure was found to expand with increasing TiO_2 due to formation of more [BO_3] units. However, the density was dominated by increase in mass of the matrix rather than the volume. The observed pattern for increasing density with increasing TiO_2 concentration agrees with the studies of Bernard et al. [5]. Additionally, the NBO were decreased from 18.5% to 12.9%, while increasing TiO_2 concentration from 2% to 20% in Ti-NBS glasses.

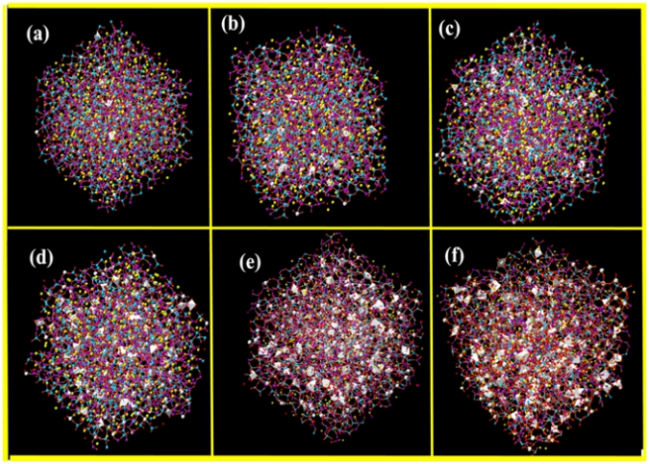

Fig.1: Snapshot of Ti-NBS glasses with (a) 1.95%, (b) 4.77%, (c) 9.10%, (d) 13.06%, (e) 16.69% and (f) 19.97%, TiO_2 concentration captured at 50ns [Si: cyan, B: purple, Na: yellow, O:red, Ti: white polyhedral].

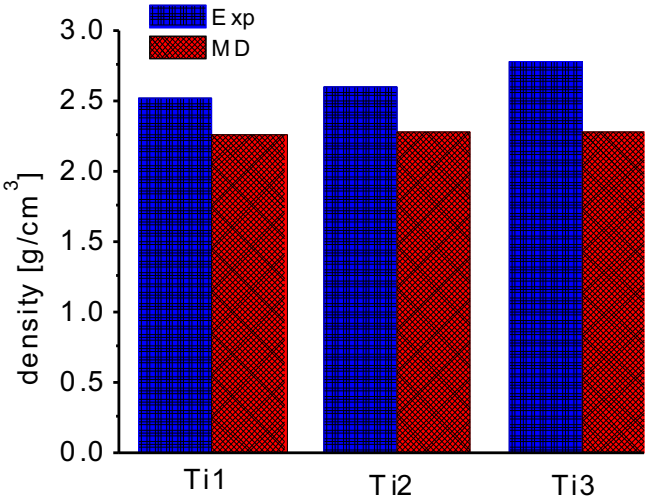

Fig.2: TiO_2 concentration effect on density of NBS glass.

Even at highest TiO_2 concentration of 20% in Ti-NBS glasses, the TiO_2 seems to be distributed throughout the glass network as shown in Fig.3(I) and Fig.3(ii). The presence of Ti-O-Ti linking along with Ti-O-Si and Ti-O-B was also observed in the simulated glasses. The snapshot of Ti-O-Ti chain is shown in Fig.3(iii) and Fig.3(vi) respectively. Interestingly, titanium ions in the glass network were observed in TiO_6 and TiO_5 structural forms. The octahedral structure of TiO_6 and square pyramid structure of TiO_5 is shown in Fig.3(iv) and Fig.3(v) respectively. Fig.3(vii) to Fig.3(x) indicate different structural forms of Ti-Ti connection, such as Ti-Ti connected with two shared oxygen atoms, and three shared oxygen atoms. To be noted, no Ti^{4+} was found in TiO_4 tetrahedral form in the Ti-NBS glasses. This shows that multi-coordinated Ti ions, do not change from octahedral to tetrahedral coordination by isomorphically replacing SiO_4 tetrahedrals. The absence of TiO_4 structural form has also been supported by the studies of Kukharenko et al. [22] as well as Osipov et al.[10].

Network Strength

The network connection was demonstrated by estimating the probable distribution for connecting network

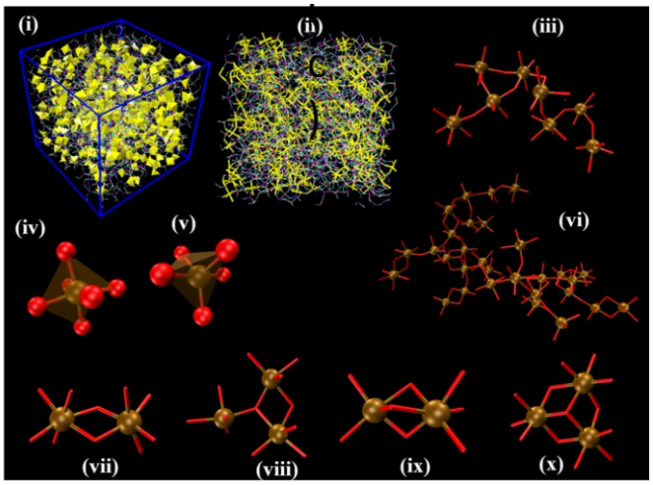

Fig.3: (i, ii) Snapshot representing the distribution of TiO_n polyhedral in the glass network, (iii, vi) images representing Ti-Ti chain network in the glass; (iv, v) TiO_6 and TiO_5 structural forms of Ti; (vii-x) Ti-Ti connectivity with two and three shared oxygen atoms.

formers with methodologies as used in our previous article[16].

The results in Fig.4 show the order of preference as Si-O-B4 > Si-O-B3 > Si-O-Si > B3-O-B4 > Si-O-Ti > B3-O-B3 > B4-O-B4 > B3-O-Ti > B4-O-Ti > Ti-O-Ti for Ti1; Si-O-B4 > Si-O-B3 > Si-O-Si > Si-O-Ti > B3-O-B4 > B3-O-B3 > B3-O-Ti > B4-O-B4 > B4-O-Ti > Ti-O-Ti for Ti2; Si-O-B3 > Si-O-B4 > Si-O-Ti > Si-O-Si > B3-O-B4 > B3-O-Ti > B3-O-B3 > B4-O-Ti > B4-O-B4 > Ti-O-Ti for Ti3; Si-O-B3 > Si-O-Ti > Si-O-B4 > Si-O-Si > B3-O-Ti > B3-O-B3 > B3-O-B4 > B4-O-Ti > Ti-O-Ti > B4-O-B4 for Ti4; Si-O-Ti > Si-O-B3 > B3-O-Ti > Si-O-Si > Si-O-B4 > B3-O-B3 > B3-O-B4 > Ti-O-Ti > B4-O-Ti > B4-O-B4 for Ti5; and Si-O-Ti > Si-O-B3 > B3-O-Ti > Si-O-Si > Si-O-B4 > B3-O-B3 > Ti-O-Ti > B3-O-B4 >B4-O-Ti > B4-O-B4 for Ti6 (B3: BO_3, and B4: BO_4).

Snapshot for connectivity of polyhedrals is shown in Fig.5. Results show that with the sufficient presence of B4 fraction (x>30%), the Si-O-B connections are favored over Si-O-Si connections. For Ti1 and Ti2, where B4 fraction is x>45%, the Si-O-B4 > Si-O-B3 > Si-O-Si order was followed, however, with B4 fraction 30% - 40%, the order was changed to Si-O-B3 > Si-O-B4 > Si-O-Si and then for B4 fraction below than 30%, it was Si-O-B3 > Si-O-Si > Si-O-B4. Our results showed abundant presence of B4-O-B4 connections.

Though all three B3–O–B4, B3–O–B3, and B4–O–B4 links were present, the probability of connecting B4-O-B4 was always minimum among the three. However, for higher B4 fraction (i.e., Ti1, Ti2 and Ti3), the intermixing of B3 and B4 i.e., B3-O-B4 connections were found to be preferred over either of B3-O-B3 or B4-O-B4 connections. On the other hand, for lower B4 fraction (system Ti4, Ti5 and Ti6), the order was followed as B3–O–B3 > B3–O–B4 > B4–O–B4. Our results are in agreement with the studies of Yu et al.[27] who showed that the presence of B_p-O-B_q motifs (p and/or q is equal to 3 and/or 4) is primarily controlled by the fraction of B4 and NBO content.

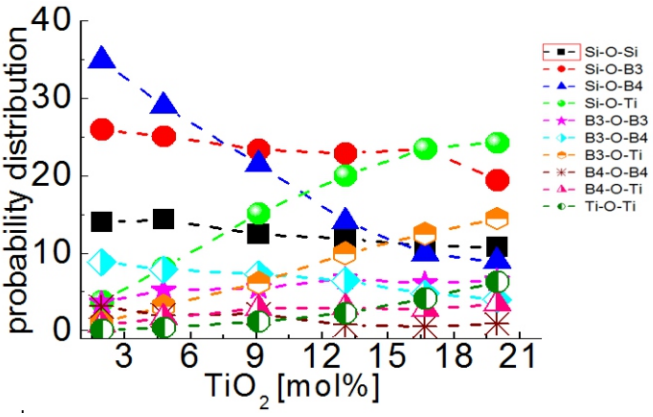

Fig.4: Probability distribution profile for preferential connection of various (X-O-X′; where X and/or X′=SiO_2, BO_3, BO_4, and TiO_n) structural units in simulated Ti-NBS glass compositions.

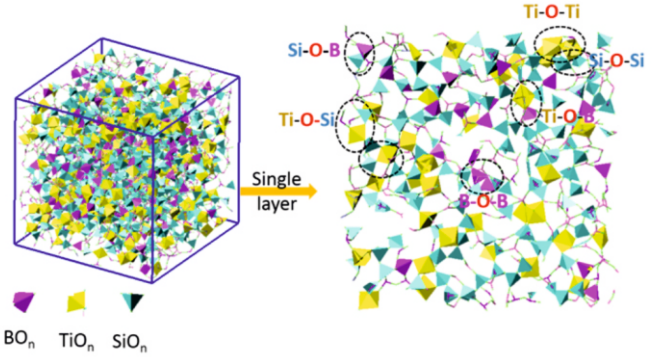

Fig.5: Image representing the connectivity of different polyhedrals in Ti-NBS glass.

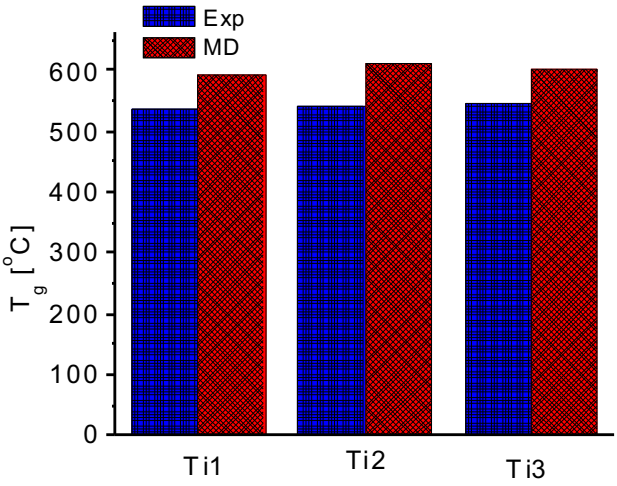

Fig.6: Effect of TiO_2 concentration on the glass transition temperature of Ti-NBS glass.

Thermal Strength

The fabrication easiness was analyzed in terms of glass transition temperature (T_g). The estimated glass transition temperature of simulated glasses is shown in Fig.6. The results show increasing Tg with TiO_2 addition in base NBS glass matrix. The same was also expected from the increasing BOs with Ti addition in Ti-NBS glasses. Though with TiO_2 addition, BO_3 fraction is increased, which is known to reduce the melting temperature, however, the increasing Tg with TiO_2 addition in Ti-NBS glasses seems to be linked with the increased strength of glass skeleton with TiO_2 doping. Hereby, results show that TiO_2 addition would increase the melting temperature during glass fabrication process.

Chemical Strength

In order to understand the chemical durability which measures the strength of the glass in contact with water, the interaction of NBS and Ti-NBS glass was studied. The glass-water system was modelled by keeping the amorphous structure of glass in adjacent to a box containing 2000 number of water molecules(TIP4P/2005 water model). The interaction between glass atoms and water molecules was estimated using Lennard-Jones potential model. The final snapshot in Fig.7 shows that some of sodium ions are diffused from bulk glass region to the interface, while few of them were migrated to the bulk aqueous phase. Mass density profiles of atoms O, Na and O_w for NBS and Ti-NBS systems are shown in Fig.8. Results show the accumulation of Na ions near the water side of interface, whereas, presence of sodium depleted zone at the glass side of interface.

Also, compared to bulk region, the density of water molecules was observed to be higher near the interface where accumulation of Na ions was noticed. This shows the structuring of water molecules and accumulated sodium ions at the glass-water interface. Also, the glass-water interface seems to be sharper for Ti-NBS than the NBS glass, may be due to reduced accumulation of sodium ions at the interface for Ti-NBS glass than the NBS glass. Apart from this, one can also observe the diffusion and accumulation of water molecules in sodium depleted zone of glass. Few water molecules were even migrated to bulk glass phase as shown by density profiles. Interestingly, water molecules were found to diffuse into glass network in its intact form. Hereby, it can be stated that water

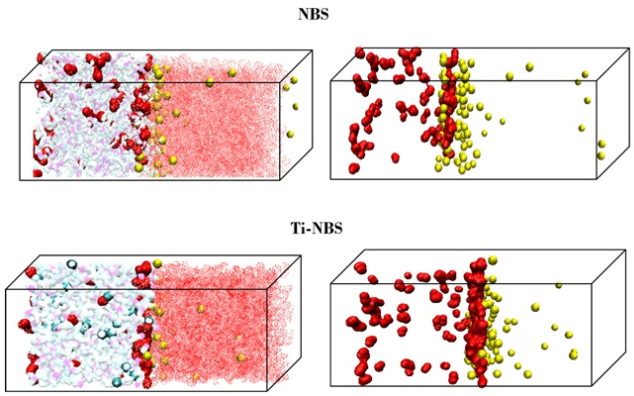

Fig.7: Snapshot representing Na leaching to interface and bulk aqueous phase, and water diffusion to glass regime for NBS and Ti-NBS glass from MD simulations [glass matrix - Si: cyan, B: magenta, Ti: cyan, Na: yellow balls; aqueous water shown by solvent style with red color; water extracted to glass side of interface and bulk glass regime shown by red quick surface style].

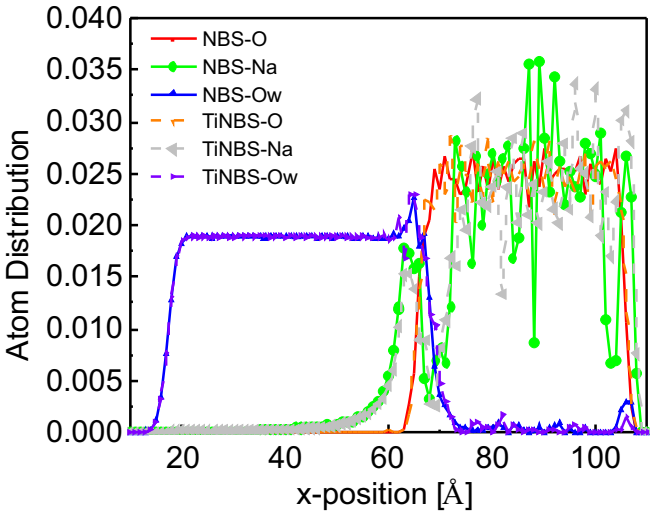

Fig.8: Atom distribution profile for O_{water}, O_{glass} and Na ions for NBS and Ti-NBS glasses.

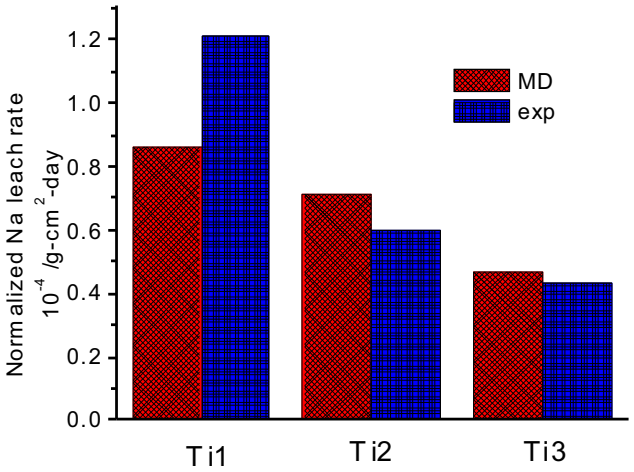

Fig.9: Effect of TiO_2 concentration on Na leach rate.

molecules can enter in the glass network without being chemically reacted with the glass network. Furthermore, the dividing boundaries of mass density profiles for atoms O and O_w were used to evaluate the interface position. The interfacial region was decided to be of 5Å thickness across the intersection point and region beyond that was considered as bulk phase of water and glass respectively. Interestingly, the adsorption of water molecules was found to affect the glass structure considerably for surface region and marginally for bulk region. The density of glass atoms was reduced by half at glass surface (0.57g/cm^3) compared to bulk region (1.36 g/cm^3).

The number of accumulated Na ions at the interface as well as the number of Na ions migrated to bulk aqueous phase was found to be considerably reduced for Ti-NBS glass compared to NBS glass (data shown in Fig.9). This leads to a significant decrease in total number of Na ions leached from the glass to aqueous solution while Ti doping of NBS glass. On contrary to sodium ions, the number of water molecules migrated from bulk aqueous phase to interface as well as the bulk glass region was found to be increasing with Ti doping of NBS glass, which might be linked with the higher concentration of alkali ions in Ti-NBS than NBS, remained after keeping them in contact with aqueous solution.

The computed results show that leaching of Na ions can be controlled by TiO_2 doping of NBS glasses. In particular, for Ti-NBS glasses, the TiO_n connected Na^+ ions are strongly attached to glass network and are less likely to move compared to free Na^+ ions in bare NBS glass matrix. As a result, Ti bearing glasses will be less prone to leaching when exposed to aqueous environment compared to Ti free NBS glasses. In other words, the chemical durability of sodium borosilicate glasses is supposed to increase with doping of TiO_2 [28].

Summary and Conclusion

The present report demonstrates that BKS potential model with the selected forcefield parameters can be utilized to simulate the glasses with multi-component oxides. Admitting the advantageous effect of TiO_2 doping for optical and nuclear waste glasses, the present studies feature the behaviour of Ti-NBS glasses as function of TiO_2 concentration in the glass matrix. The modification in glass structure, mechanical integrity, thermal strength and chemical durability was probed using molecular dynamic simulations. Results report influence of Ti doping and concentration on important properties of borosilicate glasses. The results might be very helpful in prediction of effects associated with the dopant's nature and concentration. Hereby, the present results might have great academic as well technological significance for further guidance in the selection of dopant oxide for multi-component glass for nuclear waste immobilization.

Acknowledgement

Computer division is acknowledged for providing 'ANUPAM' super computation facility. Pallavi Yevale and Annie Joseph of PSDD are thankfully acknowledged for glass experiments.

References

[1] M. J. Plodinec, Glass Technol-part A, 2000, 41, 186-192.

[2] C. P. Kaushik, Procedia Mater. Sci., 2014, 7, 16-22.

[3] Janbandhu, S. Y.; Joshi, A.; Munishwar, S. R.; Gedam, R. S. Appl. Surf. Sci. 2019, 497, 143758.

[4] Azooz, M. A.; Aiad, T. H. M. A.; ElBatal, F. H.; ElTabii, G. Indian J. Pure Appl. Phys. 2008, 46, 880-888.

[5] Bernard, C.; Chaussedent, S.; Monteil, A.; Ferrari, M. Philos. Mag. B 2002, 82, 681-693.

[6] Karlsson, S.; Bäck, L. G.; Kidkhunthod, P.; Lundstedt, K.; Wondraczek, L. Opt. Mater. Express 2016, 6, 257129.

[7] Status and Trends in Spent Fuel and Radioactive Waste Management; IAEA Nuclear Energy: Series No. NW-T-1.14: 2018.

[8] Orignac, X.; Barbier, D.; Du, X. M.; Almeida, R. M.; McCarthy, O.; Yeatman, E. Opt. Mater. Express 1999, 12, 1-18.

[9] Orignac, X.; Vasconcelos, H. C.; Almeida, R. M. J. Non-Cryst. Solids 1997, 217, 155-161.

[10] Osipov, A. A.; Korinevskaya, G. G.; Osipova, L. M.; Muftakhov, V. A. Glass Phys. Chem. 2012, 38, 357-360.

[11] Marzouk, M. A.; ElBatal, F. H.; ElBatal, H. A. Opt. Mater. 2016, 57, 14-22.

[12] Morsi, M. M.; El-Shennawi, A. W. A. Phys. Chem. Glasses 1984, 25, 64-68.

[13] Strimple, J. H.; Giess, E. A. J. Am. Ceram. Soc. 1958, 41, 231-237.

[14] S. Plimpton, J. Comput. Phys., 1995, 117, 1-19.

[15] B. W. H. v. Beest, G. J. Kramer and R. A. v. Santen, Phys. Rev. Lett., 1990, 64, 1955-1958.

[16] P. Sahu, Sk. M. Ali, K. T. Shenoy, S. Mohan, A. Arvind, G. Sugilal and C. P. Kaushik, Phys. Chem. Chem. Phys., 2021, 23, 14898.

[17] P. Sahu, A. A. Pente, M. D. Singh, I. A. Chowdhri, K. Sharma, M. Goswami, S. M. Ali, K. T. Shenoy and S. Mohan, J. Phys. Chem. B, 2019, 123, 6290−6302.

[18] B. A. Luty and W. F. v. Gunsteren, J. Phys. Chem., 1996, 100, 2581–2587.

[19] L.-H. Kieu, J.-M. Delaye, L. Cormier and C. Stolz, J. Non-Crystal. Solids, 2011, 357, 3313–3321.

[20] M. P. Allen and D. J. Tildesley, Computer Simulation of Liquids, Clarendon Press, Oxford University, 2017.

[21] Manaktala, H. K. An Assessment of Borosilicate Glass as a Highlevel Waste Form Nuclear Regulatory Commission Contract NRC-02-88-005 (CNWRA 92-017), San Antonio, Texas, 1992.

[22] Kukharenko, S. A.; Shilo, A. E.; Itsenko, P. P.; Kutsai, A. N. T J. Superhard Mater. 2010, 32, 396-405.

[23] Ruengsri, S.; Kaewkhao, J.; Limsuwan, P. Procedia Eng. 2012, 32, 772-779.

[24] Limbach, R.; Karlsson, S.; Scannell, G.; Mathew, R.; Edén, M.; Wondraczek, L. J. Non-Cryst. Solids 2017, 471, 6-18.

[25] Farges, F.; Jr., G. E. B.; Navrotsky, A.; Gan, H.; Rehr, J. J. CGeochim Cosmochim Acta 1996, 60, 3039-3053.

[26] Scannell, G.; Huang, L.; Rouxel, T. J. Non-Cryst. Solids 2015, 429, 129–142.

[27] Yu, Y.; Stevensson, B.; Edén, M. J. Phys. Chem. Lett. 2018, 9, 6372–6376.

[28] P. Sahu, Sk. M. Ali, : Langmuir 2022, 38, 7639−7663.

Improved Biomaterials

5

Zirconia Protective Coating on Ti6Al4V Bio-alloy to Improve Corrosion and Wear Resistances

Sunita Kedia*[1,4], Kiran Yadav[2], Pratiksha Pawar[2], Gumma Saradhi[3], S. Roychowdhury[3,4] and J. Padma Nilaya[1,4]

[1]*Laser & Plasma Technology Division, Bhabha Atomic Research Centre, Mumbai – 400085, INDIA*
[2]*Department of Physics, K. J. Somaiya, Vidyavihar, Mumbai – 400077, INDIA*
[3]*Material Processing & Corrosion Engineering Division, Bhabha Atomic Research Centre, Mumbai – 400085, INDIA*
[4]*Homi Bhabha National Institute, Anushaktinagar, Mumbai – 400094, INDIA*

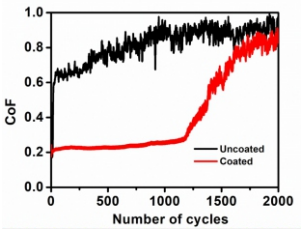

CoF versus number of cycle

ABSTRACT

Methods to limit wear and corrosion of artificial implants is crucial to reduce inflammation, allergies and implant failure. Pulsed laser deposition of zirconia thin film at a substrate temperature of 400 ^{0}C has been shown to work as protective layer on Ti6Al4V bio-alloy and improve its wear and corrosion resistances. A reduction in corrosion rate from 4.55 mil/yr to 2.89 mil/yr was observed for Ti6Al4V bio-alloy after thin film coating of zirconia. Tribological analysis indicated a reduction in wear rate of Ti6Al4V by 0.5 x 10^{-3} mm^3/Nm after zirconia coating.

KEYWORDS: *Biomaterial, Ti6Al4V, Zirconia, Pulsed laser deposition, Tribology, Corrosion*

Introduction

In an era of ever-increasing demand for artificial implants, the search for most suitable biomaterials that can be converted into desired implants such as, bone plates, screws, orthopaedic and dental devices is an ongoing effort. As defined by American National Institute of Health *"a substance or combination of substances, other than drugs, synthetic or natural in origin, which can be used for any period, which augments or replaces partially or any tissue, organ or function of the body are considered as biomaterial"* and biocompatibility of that material is its potential to perform the expected activities related to a particular remediation without producing any adverse effect locally or to the body [1]. In this regard, numerous materials such as stainless steel, titanium, cobalt, nickel and magnesium based alloys have already proven their biocompatibility [2]. Of late, Ti6Al4V-alloy of titanium has been identified as one of the most useful biomaterial for dental and orthopaedic applications because of its biocompatibility, mechanical properties, high strength-to-weight ratio and elastic modulus [3]. However, in the body environment comprising of aqueous medium, ions and biological molecules, the passivation oxide layer on the surface of Ti6Al4V is weakened causing release of harmful ions from the material due to wear and corrosion. Accumulation of wear debris and diffusion of corrosion products into the adjacent host tissue can cause inflammation, hypersensitivity and toxicity in patient body [2]. Since initial interactions and the subsequent acceptance of an implant by human body are governed by its surface properties, researchers have been working towards suitably altering the surface properties of existing biomaterials so as to make them more biocompatible. Laser induced surface modification is a method to improve tribological and corrosion properties of biomaterials [4-5]. On the other hand, coatings of oxides and carbides have also been found effective in improving corrosion and wear resistance of biomaterials [6-7]. Various coating techniques e.g., chemical vapour deposition [8], sol-gel [9], plasma based coatings [10] have been tried by many groups. Thin film coating by pulsed laser deposition (PLD) method has gain interest as the process gives control on various parameters such as, laser fluence, substrate temperature, target-substrate distance and deposition time.

In the work being presented here, PLD technique has been used for coating of zirconia thin film on Ti6Al4V bio-alloy to improve its tribological and corrosion properties. A nanosecond pulsed Nd:YAG laser was employed for PLD and the coating was performed at 400 ^{0}C substrate temperature as a uniform coating over a larger area was obtained at this substrate temperature in comparison to coating done at room temperature and at 200 ^{0}C substrate temperature. The change in morphology and wettability of the sample after coating was confirmed by surface characterization. The corrosion measurement was carried out using three electrode cell in simulated body fluid (SBF) to mimic body condition. The open circuit potential (OCP) was recorded for 2h followed by recording of electrochemical potential and impedance data. Corrosion rate of the Ti6Al4V decreased from 4.56 mil/yr to 2.89 mil/yr after zirconia coating as estimated from Tafel curve and larger radius of curvature in the Nyquist impedance curve of coated sample indicated superior corrosion resistance of the sample [4]. The tribological behavior of the uncoated and coated samples was studied in terms of coefficient of friction (CoF) and wear rate at 2N normal load using stainless steel counterpart in dry sliding condition. The wear rate of the Ti6Al4V sample decreased from 1.9 x 10^{-3} mm^3/Nm to 1.4 x 10^{-3} mm^3/Nm after zirconia coating.

Materials and Methods

The Ti6Al4V-alloy sheet of dimension (20 × 20 × 1) mm^3 with average surface roughness ~ 0.52 µm was ultrasonically cleaned in acetone, ethanol, and water. As received zirconia pellet (Merck, KGaA, Germany) of thickness 2 mm and diameter 10 mm were used as PLD target. The PLD of zirconia was performed by employing a nanosecond Nd:YAG laser (λ = 532 nm, pulse duration 6 ns, repetition rate 10 Hz: Ekspla, Lithuania), the experimental set-up is shown in Fig.1a. The laser beam was focused onto zirconia target using a 50 cm focal length lens at an angle of 45 ^{0}. The plume emitted

*Author for Correspondence: Sunita Kedia
E-mail: skedia@barc.gov.in

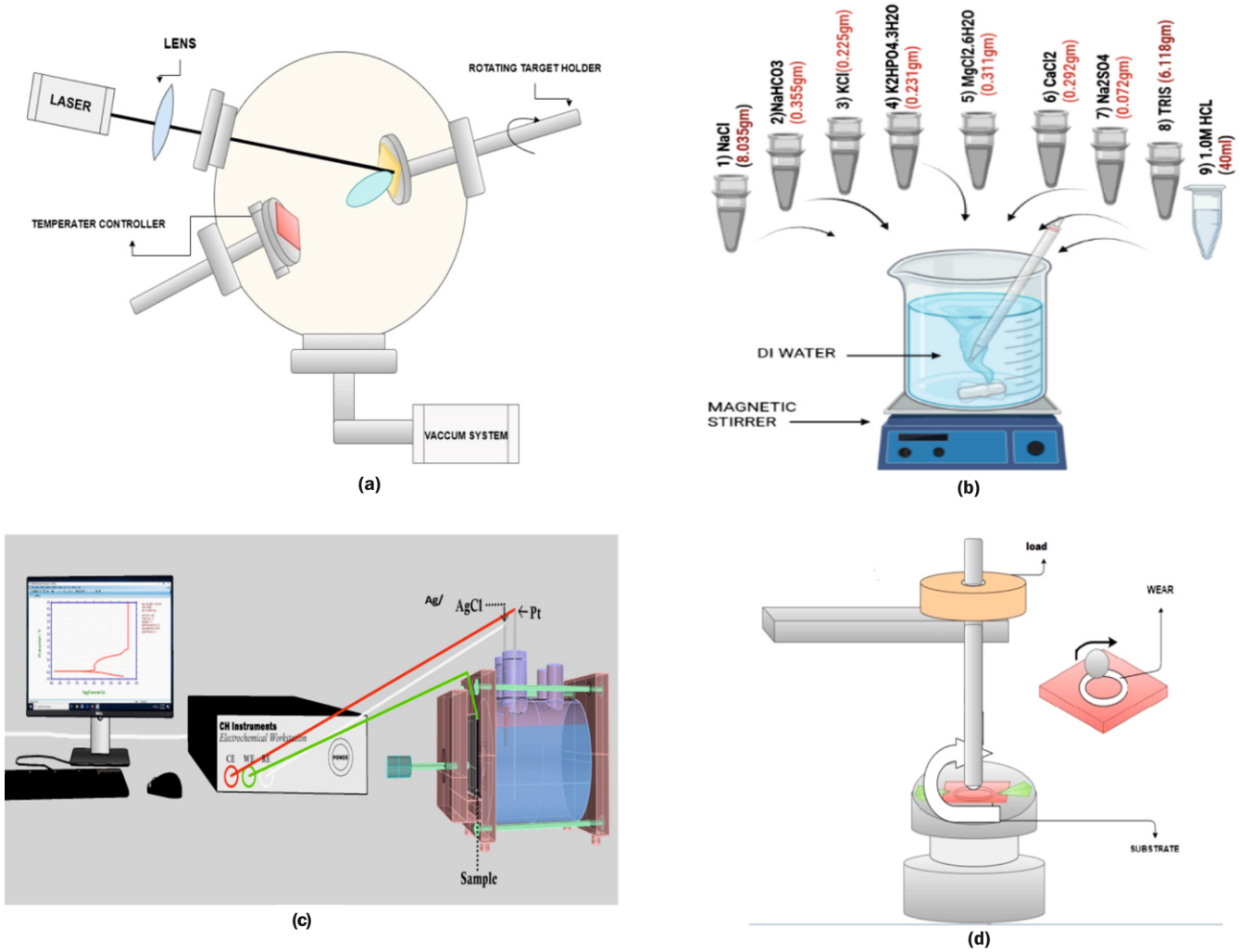

Fig.1: Experimental illustration of (a) PLD set up, (b) SBF preparation, (c) corrosion measurement and (d) Tribological analysis.

perpendicular to the target and deposited on the Ti6Al4V at 400^{0}C placed at a distance of 40mm from the target. The thin film deposition was done at laser fluence of 20 J/cm^{2} for 36000 number of laser shots. For preparing SBF NaCl (8.035gm/L), KCl (0.225 gm/L), $NaHCO_3$ (0.355 gm/L), $K_2HPO_4.3H_2O$ (0.231 gm/L), $MgCl_2.6H_2O$ (0.311 gm/L), $CaCl_2$ (0.292 gm/L), Na_2SO_4 (0.072 gm/L) and $CNH_3(CH_2OH)_3$ (6.118 gm/L) reagents were mixed in 960 ml of deionized water and 40 ml of 1M HCl by following a standard protocol, a pictorial representation is shown in Fig.1(b) [11]. Table-top Scanning Electron Microscopy (SNE, 4500M Plus, M/S. S&C, Korea) and water contact angle (VCA, Optima, India) measurements were performed to understand the topographical modification and change in wettability, respectively of the sample after zirconia coating. Micro-Raman spectrum (AIRIX Corp., Japan) was recorded to know the phase of zirconia thin film on Ti6Al4V. The electrochemical potential of the sample was measured in SBF using a three-electrode cell (CHI604E Electrochemical Analyzer, India), shown in Fig.1(c). About 0.785cm^{2} area of the sample (working electrode) was exposed to electrolyte (SBF). Platinum and Ag/AgCl were used as counter and reference electrodes, respectively. For both samples OCP was measured for 2h, the polarization curves were recorded at a scan rate 0.01V/s, over a potential range of -0.8V to 2.0V and the electrochemical impedance spectroscopy was measured in frequency range 0.1 Hz to 1MHz. The topography of the sample after corrosion studied was analyzed using 3D profilometer (CCI HD, Taylor Hobson, UK). The dry sliding wear tests were

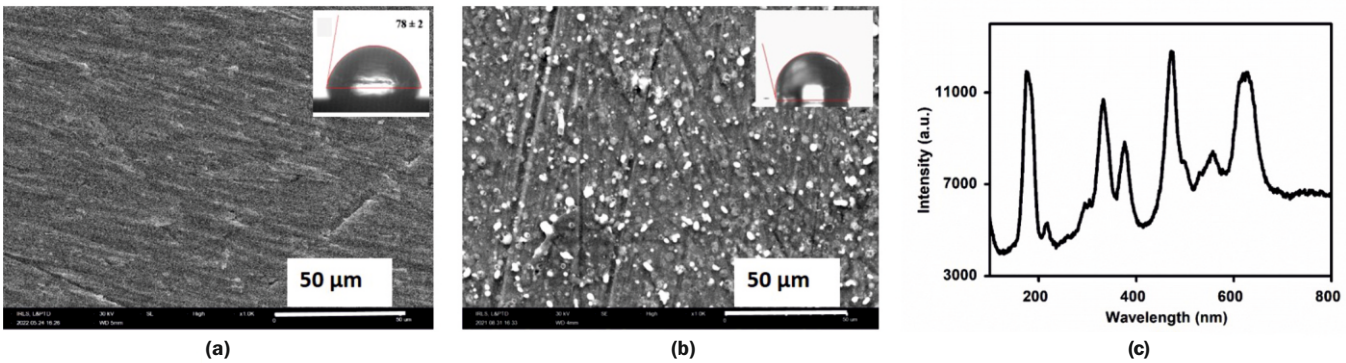

Fig.2: SEM image of (a) uncoated, (b)zirconia coated samples, inset: respective water contact angles and (c) Raman spectrum of coated sample.

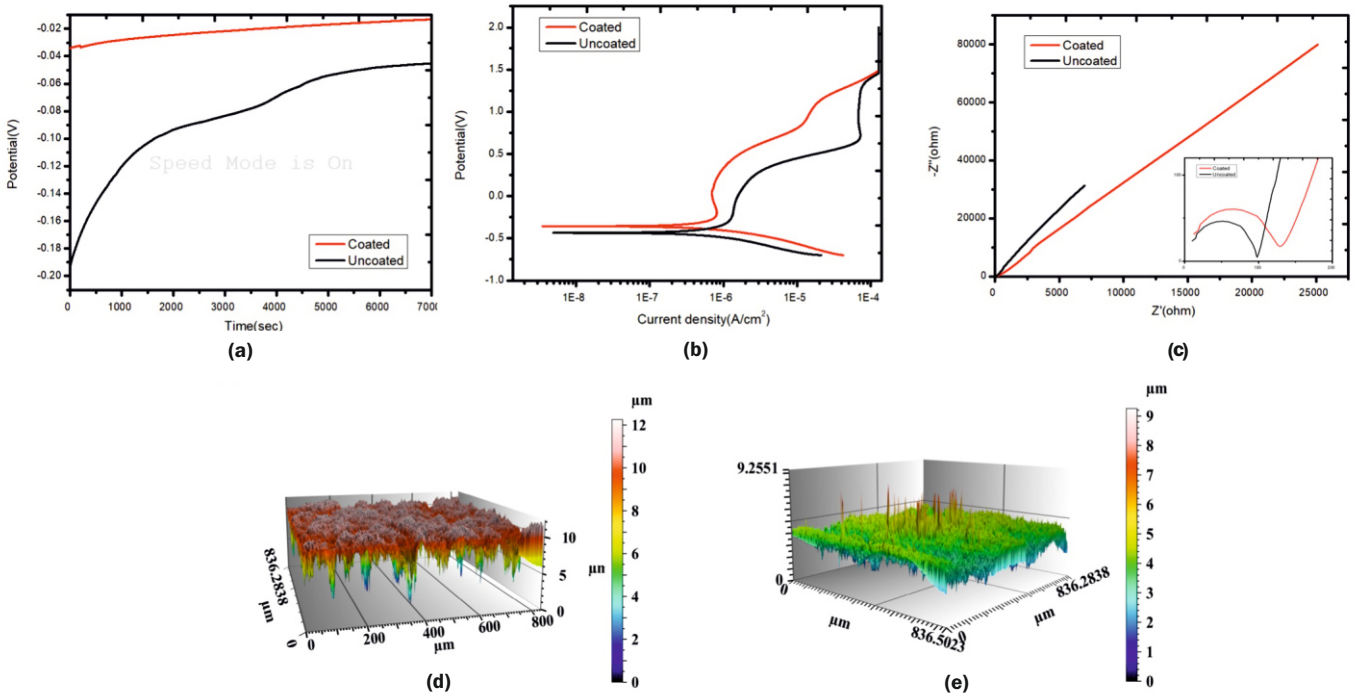

Fig.3: (a) OCP, (b) Tafel, (c) Nyquist plot of uncoated and zirconia coated Ti6Al4V (d-e) 3D Optical Profilometer image of uncoated and coated sample after corrosion measurement.

carried out by a ball-on-disc tribometer (TRB3, Anton Paar, Graz Austria) at normal load of 2N, as illustrated in Fig.1(d). A standard stainless steel ball of a diameter ~ 5 mm was used as counterpart and the measurement was done at 10Hz frequency for 2000 number of sliding cycles.

Results and Discussion

Fig. 2(a)-2(b) shows the SEM images of uncoated and coated Ti6Al4V samples in which change in morphology of the sample can be seen. As shown in the inset of the figures, the sample become hydrophobic after zirconia coating as water contact angle increased from 78^0 to 103^0. Exact thickness of zirconia coating could not be obtained due to inherent surface roughness of Ti6Al4V sample. However, the thickness was estimated to lie within 100-200 nm using 3D profilometer. In Fig.2(c), Raman peaks at 149 cm^{-1}, 224 cm^{-1}, 324 cm^{-1}, 456 cm^{-1} and 636 cm^{-1} represented tetragonal crystal structure of zirconia in the coating [12]. As shown in Fig.3(a), the OCP of coated sample showed an anodic shift in comparison to uncoated Ti6Al4V sample. An increase in OCP potential can attribute to a decrease in the anodic reaction due to growth of a passive film on the surface of the sample which indicated more stability of the coated sample in SBF environment [13]. The Tafel plot in Fig. 3b shows and increase in E_{corr} from -0.4390 V to -0.359V and decrease in I_{corr} from 5.50 x 10^{-7}A/cm^2 to 3.49 x 10^{-7}A/cm^2 for uncoated and coated samples, respectively. Since, sample with lower value of corrosion current density (I_{corr}) and higher value of corrosion potential (E_{corr}) indicates superior corrosion resistance, the zirconia coated sample has superior corrosion resistance than the uncoated sample. Corrosion rates of 4.56 mil/y and 2.89 mil/y were estimated for uncoated and coated sample, respectively. A definite decrease in corrosion rate of Ti6Al4V by half was observed after zirconia coating. In the Nyquist plot shown in Fig.3(c), the increased curvature of coated sample as compared to the uncoated one also indicates superior corrosion resistance of the coated sample. Fig.3(d)-3(e) shows the 3D profilometer images of uncoated and coated samples, respectively taken after electrochemical analysis. The large number of localized variation in depth in the surface profile of uncoated sample penetrating in to the bulk is attributable to pitting corrosion. Absence of such surface profile variations in case of zirconia coated sample shows its increased resistance to pitting corrosion in SBF environment.

Fig.4(a) shows variation in CoF of uncoated and coated sample with number of sliding cycles at normal load of 2N.

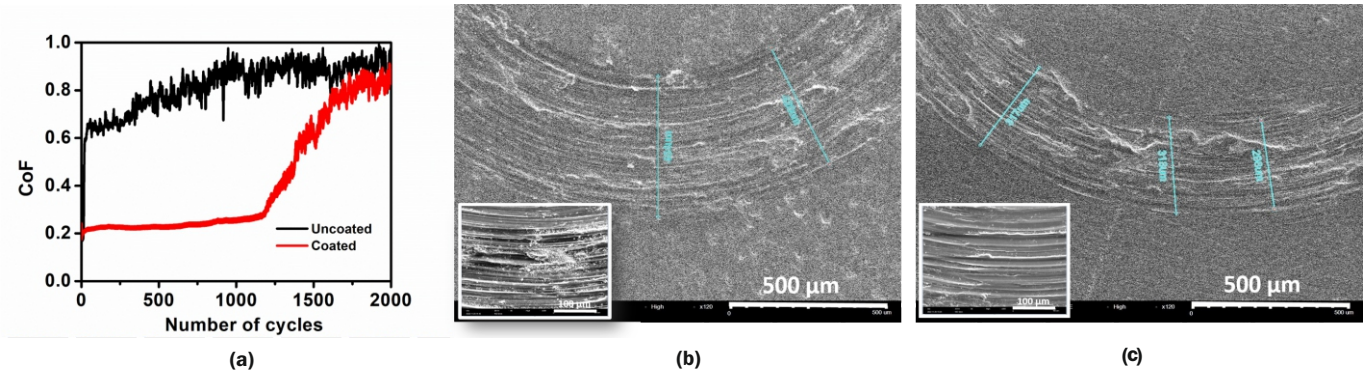

Fig.4: (a) CoF versus number of cycle and (b-c) SEM image of wear trace, inset: magnified SEM image of wear trace of uncoated (wear trace width of ~ 464µm) and coated (wear trace width of ~ 318 µm), respectively.

While CoF exhibited a sharp rise to a high value of 0.63 initially and to a value of 0.92 at the end of 2000 cycles in case of uncoated sample. For coated sample, the initial CoF was relatively low at ~0.21 which remained steady for about 1178 cycles and then, there was a gradual increase to 0.85 at the end of 2000 cycles. The maximum value of CoF in this case was found to be marginally lower than uncoated sample. These results clearly show that the coating could sustain without much alteration for a large number of cycles after which the counterpart wore out the zirconia film and CoF started increasing gradually and when counterpart penetrates the surface of the alloy a similar value of CoF as obtained for the uncoated sample by end of the cycle. The wear rate of uncoated and coated samples was estimated from the Anton-Paar software as 1.9 x 10^{-3} mm^3/Nm and 1.4 x 10^{-3} mm^3/Nm, respectively. Therefore, reduction in wear rate of Ti6Al4V by 0.5 x 10^{-3} mm^3/Nm was observed as a consequence of the protective zirconia coating.

The SEM images of wear trace in Fig.4(b)-4(c) and inset for uncoated and coated samples respectively show the formation of craters, tearing and grooves due to wear ploughing. In case of zirconia coated sample, the dominant wear mechanism is expected to be abrasive initially. As the coating wears out, the counterpart interacts with base material (Ti6Al4V) and adhesive wear mechanism will become dominant. The abrasive and adhesive nature of wear on both the samples is clearly evident from the SEM pictures. The width of wear trace was more on uncoated sample (464 µm) in comparison to coated sample (318 µm), indicating higher wear on uncoated sample as during initial wear cycles the contact area between sample and the ball is minimum and depending upon wear the contact area increases over the cycles.

Conclusion

The pulsed laser deposition of zirconia thin film modified the surface topography and wettability of Ti6Al4V sample. Anodic shift of OCP, increased E_{corr}, decreased I_{corr}, and larger impedance curvature of zirconia coated sample indicate superior corrosion resistance of the sample. Lower CoF, even grooving and lower width of wear trace point to improved wear resistance of the sample as a result of zirconia coating. Superior corrosion and wear resistance are important attributes of an implant material that lengthen its life in the body environment and this study clearly shows that zirconia coating helps improve these properties of a biomaterial.

Acknowledgment

The authors gratefully acknowledge the guidance and constant support provided by Head, Laser & Plasma Technology Division, BARC and Group Director, Beam Technology Development Group, BARC. They also acknowledge Pushpa S. Gaikwad and Nayna Jadhav, IRLS, BARC for their technical assistance during this work.

References

[1] M. Saini, Y. Singh, P. Arora, V. Arora, K. Jain, Implant biomaterials: A comprehensive review, World J. Clin. Cases., 2015, 3, 52.

[2] R. Davis, A. Singh, M. J. Jackson, R. T. Coelho, D. Prakash, C. P. Charalambous, W. Ahmed, L. R. R. da Silva, A. A. Lawrence, A comprehensive review on metallic implant biomaterials and their subtractive manufacturing, The International Journal of Advanced Manufacturing Technology, 2022, 120, 1473.

[3] M. Kaur, K. Singh, Review on titanium and titanium based alloys as biomaterials for orthopaedic applications, Materials Science and engineering C, 2019 102, 844.

[4] C. Wang, P. Tian, H. Cao, B. Sun, J. Yan, Y. Xue, H. Lin, T. Ren, S. Han and X. Zhao, Enhanced Biotribological and Anticorrosion Properties and Bioactivity of Ti6Al4V Alloys with Laser Texturing, ACS Omega, 2022, 7, 81.

[5] M. Rafieazad, J. Jaffer, C. Cui, X. Duan and A. Nasiri, Nanosecond Laser Fabrication of Hydrophobic Stainless Steel Surfaces: The Impact on Microstructures and Corrosion Resistance, Materials 11, 2018, 1577.

[6] P. Tian, X. Zhao, B. Sun, H. Cao, Y. Zhao, J. Yan, Y. Xue, H. Lin, S. Han, T. Ren and C. Wang, Enhanced anticorrosion and tribological properties of Ti6Al4V alloys with Fe3O4/HA coatings, Surface and Coatings Technology, 2022, 433, 128118.

[7] B. Ege, I. Duru, A. Kamali and A. Boccacini, Nitride, Zirconia, Alumina and Carbide coatings on Ti6Al4V femoral Heads: Effect of deposition Techniques on Mechanical and Tribological Properties, Advanced Engineering Materials, 2017, 19, 00177.

[8] G. Heinrich, T. Grijgler, S. M. Rosiwal, R. F. Singer, CVD diamond coated titanium alloys for biomedical and aerospace applications, Surface and Coatings Technology, 1997, 514, 94-95.

[9] S. Zang, C. Wang, W. Liu, Characterization and tribological investigation of sol-gel ceramic films on Ti-6Al-4V, Wear, 2006, 260, 379.

[10] B. Tang, P. Wu, X. Li, A. Fan, Z. Xu, J. Celis, Tribological behaviour of plasma Mo–N surface modified Ti–6Al–4V alloy, Surface and Coatings Technology, 2004, 179, 333.

[11] T. Kokubo and H. Takadama, How useful is SBF in predicting in vivo bone bioactivity? Biomaterials, 2007, 27, 2907.

[12] S. N. Basahel, T. T. Ali, Mokhtar, and K. Narasimharao, Influence of crystal structure of nanosized ZrO_2 on photocatalytic degradation of methyl orange, Nanoscale Res. Lett. , 2015, 10, 73.

[13] R. Hsu, C. Yang, C. Huang, Y. Chen, Electrochemical Corrosion Properties of Ti–6Al–4V Implant Alloy in the Biological Environment, Material Science and Engineering, 2004, 380, 100.

Isotope Separation

6

Atomic Vapour Diagnostics Using Tunable Diode Laser-based Absorption Spectroscopy

G. Sridhar*, S. K. Agarwalla, Das Dev Ranjan, Dileep Kumar V., A. Nagaraj, S. P. Dey, Anupama Prabhala and Sanjay Sethi
IPDS, ATLA-F, Beam Technology Development Group, Bhabha Atomic Research Centre, Mumbai – 400085, INDIA

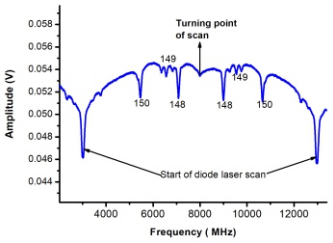

Absorption spectrum for 8° vapour divergence

ABSTRACT

In this paper we are presenting our recent results based on the diode laser-based absorption spectroscopy of weak atomic transition of Sm atoms carried out in the process chamber utilized for laser based medical isotopic separation. Identification of the isotopes, Doppler spectral width along with the level population of atoms involved in the process were successfully evaluated.

KEYWORDS: *Tunable diode laser absorption spectroscopy (TDLAS), Atomic vapour Characterization, Doppler width, Atom number density, Atomic vapour laser isotope separation*

Introduction

Collimated atomic and molecular beams finds applications in various research activities such as study of laser-atom interaction in laser spectroscopy, plasma physics and collision physics. Beam Technology Development Group, Bhabha Atomic Research Centre (BARC) is pursuing the development of the Atomic Vapour Laser Isotope Separation (AVLIS) process for separation of ^{152}Sm, ^{176}Yb and ^{176}Lu from natural feed for medical applications. The important parameters for characterizing the atomic beam are its atom number density and spectral width. Atom number density of atomic vapor has been estimated coarsely using techniques like gravimetric and source temperature based vapour density estimation. Diode laser-based absorption method is an elegant method to estimate the atomic vapour density, level population densities, spectroscopic information such as Doppler width of the transition and Isotopic shifts and HFS splitting of isotopes under study[1]. In this paper, we present tunable diode laser-based absorption spectroscopy of (spin forbidden) transition of samarium with weaker cross-section for the estimation of Doppler width, atomic level population and total density of samarium atoms in the process vapour generator. This technique can be used as a diagnostic tool for characterizing new atomic vapour source generator and online atomic vapour diagnostics for Samarium LIS process.

Experimental Setup

The experimental setup for the diode laser absorption study of samarium neutral atom is given in Fig.1(a). Commercial diode laser from Sacher Lasertehnik Littman series (TEC-500 model) at 686.093 nm was used as a probe laser for the absorption study. Samarium vapour are generated from a radiatively heated linear evaporating source. Three linear sources of 50 mm length at pitch of 70 mm are used together to generate vapour of ~200 mm length in the laser-atom interaction zone. Samarium Source in crucible was heated around 800°C in a high vacuum chamber and the emanating atomic vapor was collimated using a series of four collimators. External Cavity Diode Laser (ECDL) at 686.093 nm connects transition from metastable state at 292.58 cm^{-1} (^{7}F$_1$) above the ground state to ^{9}F$_1$ transition of samarium atom as shown in Fig.1(b). The transmitted signal was measured with photo diode (PD) and lock-in amplifier was used to detect the phase-lock detection of the amplitude modulated PD signal. As the laser frequency scanned across the transition of Sm atom,

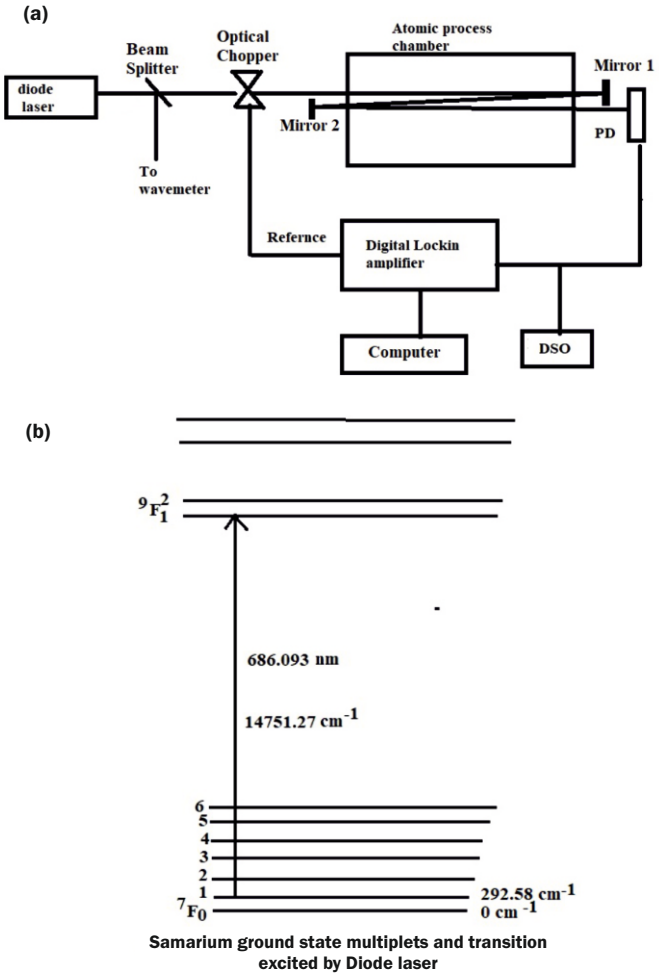

Fig.1: (a) The experimental setup. (b)Transition for absorption study.

*Author for Correspondence: G. Sridhar
E-mail: gsridhar@barc.gov.in

absorption dips in the transmitted intensity were observed corresponding to transitions of isotopes and their HFS components. The percentage of absorption depends on the product of lower level population density, absorption cross section and length of interaction. The probe laser intensity is kept below saturation intensity ($h\nu/\sigma\tau$) of the transition to avoid intensity depended nonlinear absorption. Here symbol ν is the frequency of probe laser, σ and τ corresponds to absorption cross-section and radiative life time respectively.

ECDL wavelength was tuned by providing triangular pulses to PZT transducer attached to wavelength tuning mirror of grazing incidence cavity. Corresponding wavelength/ frequency scan without any mode hop or frequency jump was monitored with help of wave meter of WS-6 model from High Finesse. The population distribution of samarium atoms in ground state and its nearby metastable septets, at a particular source temperature, was evaluated using Boltzmann distribution. As the multiplets are closely spaced in energy, the appreciable population of higher levels at higher temperature is expected. For near operating temperature for Laser Isotope Separation (LIS) process, $^7F_1$ has more population followed by $^7F_2$ and ground state $^7F_0$. Samarium has seven isotopes with even isotopes of 154,152, 150, 148 and 144 and two odd isotopes of 149 and 147 with nuclear spin of 7/2. Diode laser experiments in the wavelength region of 630- 690 nm reported in literature were carried with higher number densities of ~10^{12} per cc using heat oven pipe of longer source length (~100 cm) for measurable absorption signal for Samarium [2,3]. In the process chamber of Sm isotope separation used in this study has nominal number density of ~10^{11} per cc and 21 cm of atomic vapour length [4]. The expected absorption is less than 1%, due to low value of absorption cross section (~10^{-15}cm^2) of the transition. Hence, the experiment was designed with three optical pass configuration to obtain good signal to noise ratio of the absorption signal.

Results & Discussion

Fig.2 shows the lock in amplifier output for the vapour source with half angle divergence of 8°. Fig.3 shows simulated absorption cross-section spectrum for the transition at 686 nm for all isotopes along with various Doppler widths (100 MHz & 250 MHz) with available data on isotopic shift, Einstein's A&B coefficients, or Oscillator strengths (f_{osc}) [5], hyperfine splitting and the natural abundance. The peaks of two isotopes with even mass numbers i.e. ^{150}Sm and ^{148}Sm have been identified, along with well resolved HFS signal of ^{149}Sm with its three components in Fig.2 by comparing with simulated spectral

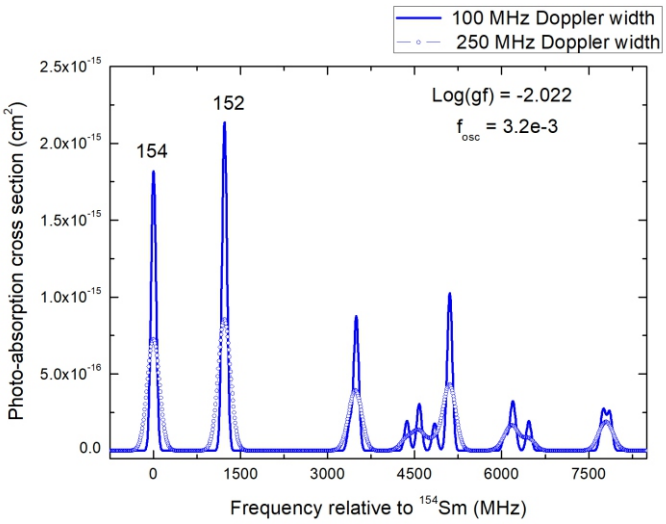

Fig.3: Simulated absorption spectrum at 686 nm.

signatures shown in Fig.3. The frequency separation between ^{150}Sm and ^{148}Sm (1616 MHz) is used as frequency marker for this spectrum and the time base was recalibrated to frequency and shown in the Fig.2.

Even isotope Sm-148 was fitted with Gaussian function and the spectral width of 92 MHz and peak absorption is ~4.89% was evaluated for three pass configuration. Here, Doppler width is dominant broadening mechanism over natural width of ~0.449 MHz as reported. Doppler spectral line broadening is an important process parameter for optimization of laser atom interaction[6] for high ionization yield of target isotope with high spectroscopic selectivity.

Diode laser absorption experiment was repeated for vapour source with half-angle divergence of ~18°; which is expected to have higher vapour utilization of the evaporated vapour. Increased Doppler width is expected for atomic beam with 18° half angle divergence which results in reduced peak absorption. Hence, the transition resonance is shifted from "Sm-150 & Sm-148" pair to "Sm-154 & Sm -152" pair of transition due to their higher abundance.

By red detuning the diode laser from centroid of the transition (Fig.3), we could capture three isotopic peaks with very good signal to noise ratio. Fig.4 shows the three pass absorption spectra with the vapour source at 835°C and with half-angle divergence of ~18° and at the interaction height 25 mm to 35 mm from the collimator. Comparing with the

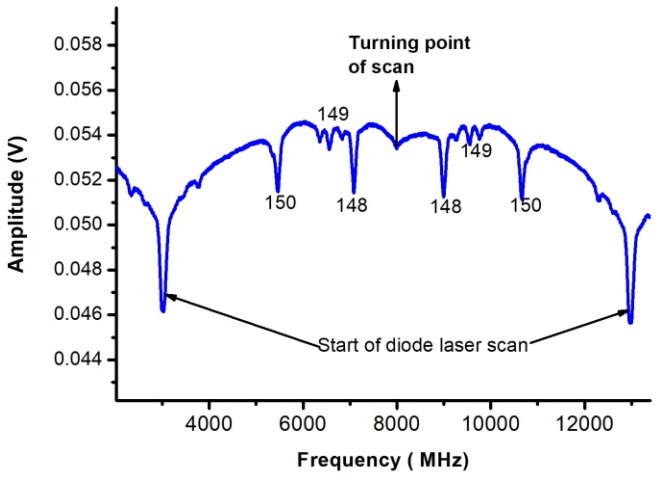

Fig.2: Absorption spectrum for 8° vapour divergence.

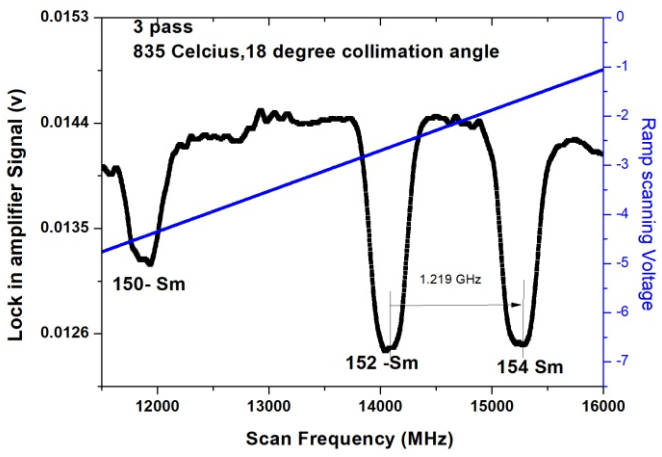

Fig.4: Three Pass Absorption spectra with 835°C of half angle of divergence of 18°.

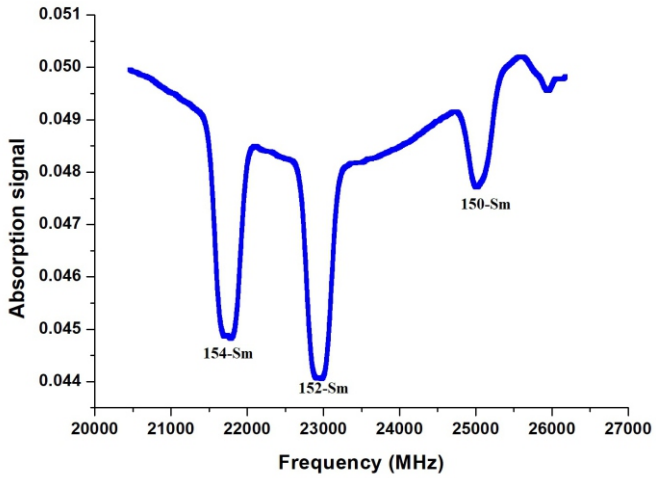

Fig.5: Two-pass absorption spectra at ~25 mm height.

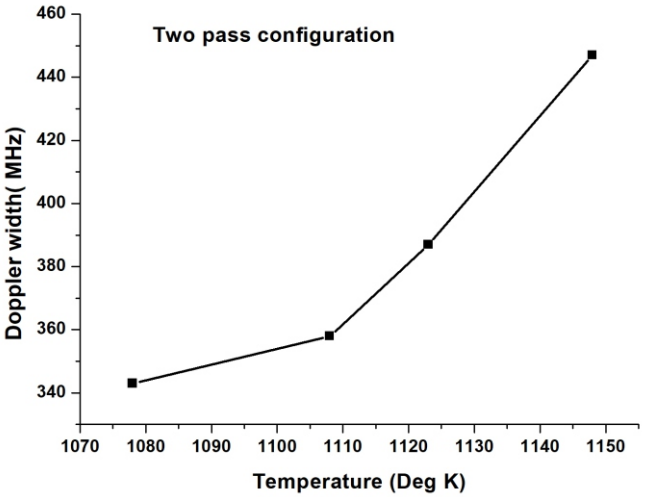

Fig.6: Doppler width Vs temperature.

simulated spectrum with position and amplitude, the peaks of 150-Sm, 152-Sm and 154-Sm were identified. The peak absorption of ~15 % for Sm-152 was obtained in a 3-pass configuration; which depends on the isotopic abundance, Doppler width and atom density. Considering all the contributions between Sm-148 and Sm-152, may be concluded that the increased peak absorption due to enhanced atom number density resulted in three-fold increase in absorption signal of Sm-152. Doppler width was estimated with Gaussian fitting from the absorption spectrum to be ~330 MHz. The peak absorption signal at Sm-152, in single pass configuration, was measured to be ~4%.

With 18-degree half angle for vapour, the absorption spectra were also obtained with two pass optical configuration, as shown in Fig.5 at 835^{0}C of source temperature. Study of Doppler width and estimation of number density with four sets of temperature were carried out. The absorption signal, using two-pass optical configurations is measured to be ~10%. Effect of temperature on Doppler width was studied and is plotted in Fig.6 for Sm-152 isotope.

From the measurement of Doppler width and peak absorption (transmission), atom number density of the levels involved in the transition can be estimated using equation(1)[7].

$$k_{\vartheta 0} = \left(\frac{2}{\Delta\vartheta}\right)\left(\frac{\ln 2}{\pi}\right)^{\frac{1}{2}}\left(\frac{\lambda^2}{8\pi}\right)\left(\frac{g_2}{g_1}\right)N\ A \qquad (1)$$

Where K_{v0} is the absorption coefficient at the peak, which can be calculated from Beer-Lambert's law of absorption. Doppler width (Δv) and peak absorption estimated from the Gaussian fitting of individual isotopic (even) absorption profile. The constants g_1 and g_2 are degeneracy parameter of the lower and excited state for this J 1→1 transition. The constant A in equation 1 is Einstein's 'A' coefficient[3,5] for the transition is reported in the literature as 0.4487x10^{5} sec^{-1}.

From above equation, population at J=1 of ground state septet is estimated. From level population, isotopic populations derived and further based on the even isotope abundance, total population densities have been estimated. Fig.7 shows the variation of number density as function source temperature measured by DLAS method, which displays an increasing trend as expected.

Conclusion

Here, we have presented diode laser-based absorption technique as the diagnostic tool for samarium atomic vapour characterization for Samarium-LIS process chamber. As the absorption cross-section is very weak for samarium atom in the available diode laser wavelengths, we have used multi-pass configurations to achieve a good absorption signal. Important LIS process parameters such as Doppler width, available atomic level population and total atomic number density were

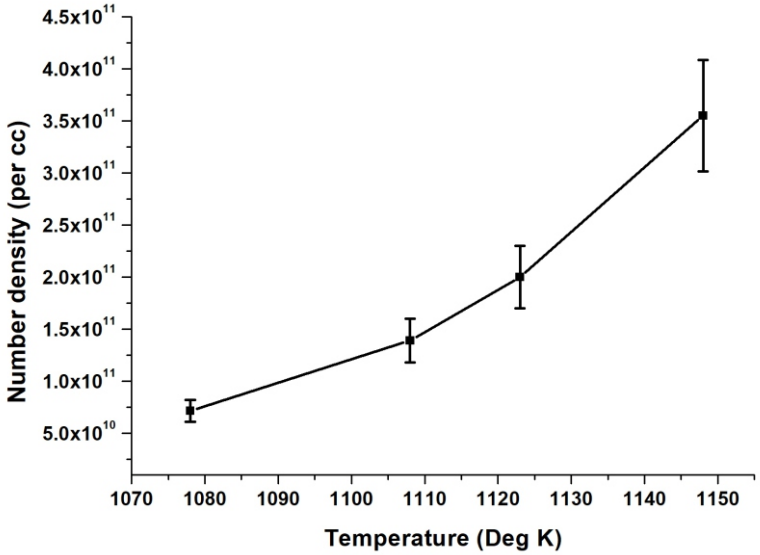

Fig.7: Total atom number density VS Temperature.

evaluated. With 18 degree half angle divergence of atomic vapour, absorption signal was obtained with Sm-152 in single pass configuration itself, firmly establishes that this technique can be adapted for online neutral density measurement for Samarium LIS process.

Acknowledgements

Authors acknowledge the support and encouragement of Director, Beam Technology Development Group, BARC. The entire team of ATLA-F, BTDG is acknowledged for their help in the form of providing resources used in the experiments. Authors also thank Ajay Kasbekar, EmA&ID for providing digital lock-in amplifier developed in-house for the experiment. Fruitful discussions with P. V. Kiran Kumar, NCCCM, Hyderabad are also duly acknowledged.

References

[1] Paul Oxley et al., Precision atomic beam density characterization by diode laser absorption spectroscopy, 2016, Rev.Sci. Instrum., 87, 093103.

[2] Hyunmin Park et al., Isotope shifts of Sm I measured by diode laser based Doppler free spectroscopy, 1999, J. Opt. Soc. Am. B, 16, 1169.

[3] N. N. Kolachevskii et al., Isotopic shifts and the hyperfine structure of Samarium spectral lines at 672 and 686 nm, 2001, Atomic Spectroscopy, 90, 201-207.

[4] S. P. Dey, K. Karmakar, Dileep Kumar V, Tarang Garg and Sanjay Sethi, 2022, BARC Newsletter, 381, 18-20.

[5] 1995 Atomic Line Data (R.L. Kurucz and B. Bell) Kurucz CD-ROM No. 23. Cambridge, Mass.: Smithsonian Astrophysical Observatory.

[6] P. V. Kiran Kumar, G. Sridhar, Effects of laser bandwidths and Autler-Townes doublet peaks of neighboring isotopes on the ionization line shape of 168Yb isotope, 2022, 277, 107995.

[7] Gomide J. V. B et al., Construction of atomic beam system and efficient production of metastable states, 1997, Brazilian. Journ. Phys., 27, 226.

Photoisomerism in Confinement

Multiple Effects of a Nanocavity on Photoactive Guest Dynamics

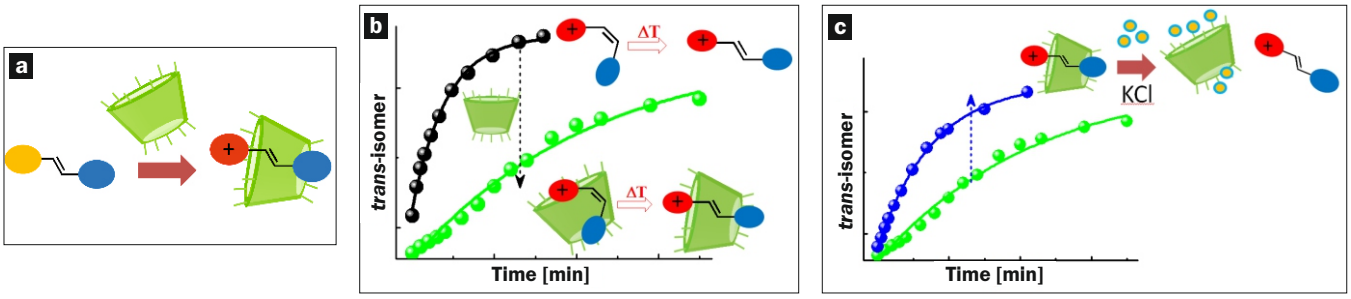

Schematics of host (SCD) induced guest (DSP) protonation (a), retardation in the kinetics of cis-trans isomerization of DSP upon complexation by SCD (b) and stimuli responsive disruption of host-guest complexation accompanied by reversal in the kinetics of cis-trans isomerization by addition of KCl.

Sharmistha Dutta Choudhury
Radiation & Photochemistry Division, Chemistry Group,
Bhabha Atomic Research Centre, Mumbai 400 085, INDIA

Macrocyclic confinement unlocks the photoisomerization potential of a guest dye, stabilizes the *cis* isomer and also imparts stimuli response, all of which are important for design of novel photo functional materials.

Photoactive molecules that undergo reversible changes in their geometry, structure or colour upon exposure to light are integral to many biological processes including vision, phototaxis and generation of proton-motive force. Moreover, photoisomerization and photochromism are important phenomena that find useful applications in areas like optical storage; light operated molecular machines and photo-pharmacology. Nature has achieved remarkable efficiency and control over its light-driven biological functions by spatial confinement of photoactive species within special pockets created in active sites of proteins. Learning from nature, chemists also seek to manipulate light induced phenomena and obtain the desired optical response by encapsulation inside different kinds of synthetic nanocavities.

In a recent study (S. Dutta Choudhury, *Langmuir* 38, 2022, 14819), it has been shown that confinement of the photoactive hemicyanine dye, *trans*-4-[4-(dimethylamino)styryl]-1-methylpyridinium iodide (DSP) within an anionic β-cyclodextrin macrocycle, sulfated-βCD (SCD), produces multiple interesting effects on its reversible *trans-cis* isomerization process. Interestingly, under normal conditions DSP is inactive toward photoisomerization due to a fast alternate pathway of nonradiative relaxation via formation of twisted intramolecular charge transfer state. However, on protonation of DSP, the intramolecular charge transfer pathway is blocked and its photoisomerization potential can be revived. It is found that the SCD macrocycle plays an important role in this regard by influencing the protonation equilibrium of DSP. The greater affinity of the anionic SCD host for protonated DSP compared to the unprotonated form, leads to "host assisted guest protonation", which provides the desired impetus for unlocking the photoactivity of DSP.

Importantly, the encapsulation of DSP by SCD not only activates the *trans-cis* isomerization of the dye but also significantly retards the thermal back conversion of the *cis* isomer to the *trans* isomer. This is brought about due to stabilization of the *cis* isomer inside the macrocyclic host by geometrical confinement as well as favourable electrostatic interactions. Furthermore, the contribution of electrostatic effects on the host-guest interaction also makes it possible to tune the kinetics of reverse *cis-trans* isomerization of DSP with the help of external stimulants. A simple additive like KCl is found to disrupt the host-guest complexation and consequently influence the recovery of the *trans* isomer of DSP. The SCD induced stimuli responsive, reversible isomerization of DSP is certainly an interesting case from the perspective of chemical sensing or light operated functional materials with host-guest systems.

Pulse Capacitor Development Facility at CnID, BARC, Trombay

Technology of High Voltage Pulse Capacitor

Greater indigenization in advanced technology domains in spirit of 'Atmanirbhar Bharat'

*Ravindra Kumar Sharma, Manohar A. Gurav, Satish G. Chavan, Vikas Kurariya, Anant Ram, Vivek Sanadhya, Anuradha Mayya and Siddhartha Mukhopadhyay

Electronics and Instrumentation Group, Bhabha Atomic Research Centre, Mumbai 400085, INDIA

The technology of high-voltage (HV) low-inductance capacitors has numerous applications in domains such as fast x-ray and neutron sources, lasers, high power microwave generators, electron beam accelerators, plasma generation and electromagnetic welding in materials, industry, medical appliances, scientific R&D, nuclear energy, space and defense sectors. By virtue of fast discharge and low footprint, high current film-foil capacitors are amongst the most-sought-after technologies in the day-to-day working of scientific R&D centres and also industries.

However, their availability in the domestic market remains a key concern. This issue could be addressed through incorporating advanced electrical designs and fabrication processes in the existing capacitor industry to achieve desired characteristics, including low inductance, high energy density, high current capability and enhanced lifetimes.

Foils made using pure aluminium and bi-axially oriented 'hazy' polypropylene films (for absorption of impregnating oil) are wound in alternate layer configuration. This is in tune with the design specifications worked out in BARC for new extended foil & internal series configurations. The capacitor elemental windings of film-foil were carried out on a custom-made seven-segment internal series automatic capacitor winding machine and a semi automatic machine in Class 10000 environment. Film-foil rolls were placed in the respective feeders as per the design configuration. Round and flat elemental windings were developed using split mandrel technique.

The newly developed process for "On-line" impregnation capacitor winding is preferred for oil-free (dry) capacitors. A low viscosity electrical grade thermally curable epoxy resin was utilized as an impregnant during elemental winding. Interconnections of elements were prepared using high power soldering set-up for high peak currents and crimping of conducting foils for up to 10 kA applications. Thicker copper strips (up to 400 μm) were used for electrical connections during soldering between two series/parallel capacitor

Pulse capacitors of various ratings and configuration developed at CnID.

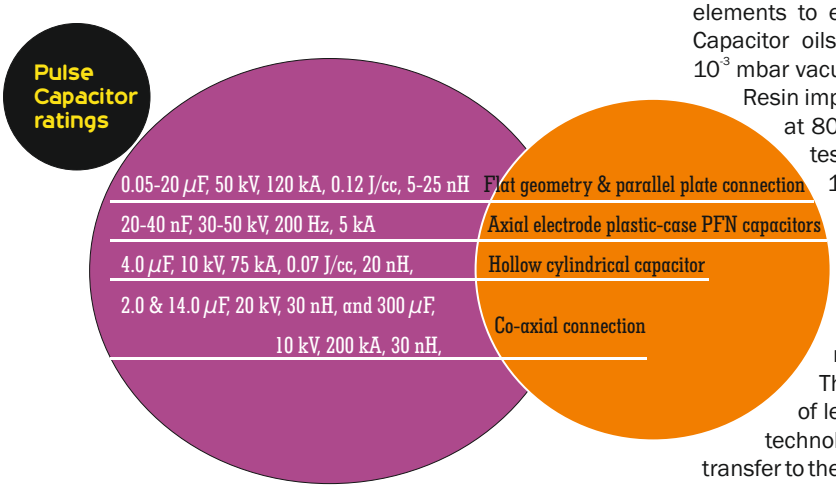

elements to ensure low resistance and mechanical rigidness. Capacitor oils functioned as an impregnating medium under 10^{-3} mbar vacuum in an oil impregnation-cum-heating pilot plant. Resin impregnated capacitor elements were thermally cured at 80°C for three hours. The fabricated capacitors were tested electrically as per "Bureau of Indian Standard 13666". More importantly, this technology - developed in-house - had been utilized and supported through test results of various bespoke designs and fabricated capacitors as per the requirements of APPD, APD & CnID users in BARC. Pulse capacitors were fabricated and utilized with a maximum rating of 100s of kA and life of 10^7 shots. These capacitors also have extremely low inductance of less than 50 nH and resistance of up to 30 mΩ. The technology of low inductance pulse capacitor is ready for transfer to the Indian industry.

Authors deeply acknowledge the support provided by the CnID, RCnD, TSD, APPD, APD in BARC. Special thanks to R. K. Sadhu, Ex-head, ATSS, E&I Group and Archana Sharma, Director BTDG, BARC, for their fruitful discussion and guidance during the project activity.

*Author for Correspondence: Ravindra Kumar Sharma
E-mail: rksharma@barc.gov.in

RIVERINE SYSTEMS

Hydrological, Hydrosocial and Hydro-heritage Dynamics

By Tirumalesh Keesari*

Riverine Systems – Understanding the Hydrological, Hydrosocial and Hydro-heritage Dynamics
Editor: Abhijit Mukherjee
Springer International Publishing, January 2022

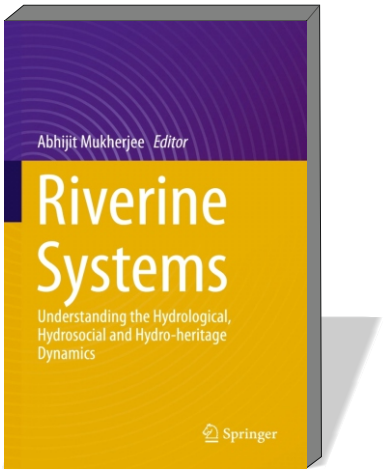

Being an ardent researcher in the field of environmental science, applied geology and geochemistry, Prof. Abhijit Mukherjee has edited this very important, useful and timely publication on 'Riverine Systems' providing a unique opportunity to integrate the knowledge on regional-scale riverine reviews to local-scale case-studies, ranging from availability to pollution, national-level river management to transboundary governance. Prof. Mukherjee has to his credit two books, "Groundwater of South Asia" (Springer) and "Global Groundwater: Source, Scarcity, Security, Sustainability, Solutions" (Elsevier) as lead editor those were well appreciated by both domestic and foreign scientific fraternity. With the kind of riverine network India is endowed with (14 major rivers each of which having catchment area of ~ 20000 km^2 and above) and the instrumental role it played in nurturing the civilization of the Indian sub-continent, this publication on specifics of riverine systems is an eagerly awaited one and has the potential to boost the scientific spirits for enhanced research in riverine systems.

With a vast experience in articulation of the scientific issues and also being one of the top 50 leading scientists of India under the age of 50 years, Prof. Mukherjee has performed this herculean task of detailing the connect between the science of rivers and its history and socio-politics and well-articulated the due credence of rivers from ancient civilizations to modern human societies. A total of 23 chapters are presented in this book by leading experts and researchers from across the globe focusing hydrology, hydrosocial and hydro-heritage aspects, thus providing a much-needed knowledge on the river studies for historians, scientists, planners, social scientists and policymakers.

A major share of the book deals with hydrology of rivers, looking at their geography, fluvial processes, environmental attributes and planning through sustainable management of freshwater environments by planners, agriculturalists, industrialists, conservationists and engineers. Under this section, vulnerability and resilience status, flood hazard, effect of changing climate, natural and anthropogenic impacts are covered through case studies from various basins across India. An important aspect of environmental flow was detailed by Jain et al. in the first chapter covering very important river systems of Indo-Gangetic Plains. Further, authors provide practical and simple guidelines for future environmental flow assessments. Rajesh et al (chapter 12) describes the environmental flow impacts on water quality and utility of flow duration curve and runoff index for assessing low flow events. The status of pollution and rejuvenation of river Ganga has been a hot topic since a long time in India, authors Simon and Joshi (chapter 2) provide a very critical information on this aspect and from the lessons learnt through few global river rejuvenation attempts, the authors very carefully recommend the interventions needed for strengthening the rejuvenation program for river Ganga. Not much information is available for North-eastern parts of India with regard to vulnerability and resilience of river systems. Thakur et al (chapter 5) chose Brahmaputra river to highlight the water demand, impact of urban bodies, emerging contaminants and climate change on river system. The authors construe that existing approaches and improvement programmes by the policy makers have not yet perceived the change in climate as a critical factor and the impact it can have on the hydrogeological features and socio-economic dynamics of entire north-eastern India.

The climate change impacts are discussed for Western Himalayas by Lone et al(chapter 8) who used environmental isotopes to confirm that snow melt contributes up to 58% of river discharges. Another very interesting river pollution study was articulated by Ramya Priya and Elango (chapter 9) on Cauvery River Basin that flows across four southern states of India. The nature of aquifers and their relationship with Narmada-Sone Lineament in Narmada River Basin was dealt by Sudarshan Sahu (chapter 10).

The four chapters on hydrosocial exposition help to reorient human approach of studying rivers as an object, to understand water as being integrally embedded in its social

Dr. Tirumalesh Keesari is a Scientific Officer-G in Isotope Hydrology Section of Isotope Radiation and Application Division (BARC) and also Associate Professor in Chemical Sciences (HBNI). His research interests include water contamination, geochemical modeling,groundwater recharge, spring revival in Himalayan regions, coastal salinity and studies on extreme climatic regions of India through application of isotope technologies. He has over 90 international journal publications to his credit and also a recipient of IANCAS Tarun Datta Memorial Award, DAE Science and Technology Award and Indo-US Science and Technology Award.

context to adjust to human agencies, power asymmetries, and fostering socially-just solutions. In my view, water-human nexus study in large riverine islands of India, Bangladesh and Vietnam by Kumar et al. (chapter 14) is very informative. This chapter provides alternatives that explicitly account for plausible and co-evolving trajectories of socio-hydrological system, which further yield both insights into cause–effect relationships and help stakeholders to identify safe functioning space. The gravity of concern about interlinking rivers (ILR) in India is huge and quite evidently has been associated with acrimonious debates. Ghosh and Modak (chapter 15) articulated this aspect through tenets of the new emerging paradigm and argue that given the constraints, it does not seem that a project of this mammoth proportion will really be sustainable. The authors go on to highlight the previous instances from USA and UK in support of their interpretation/argument. Jayant Basu (chapter 16) details the issues in transboundary river water sharing pertaining to Teesta river and suggests, Nature Based Negotiated Approach (NBNA) for addressing transboundary conflicts including those in South Asia.

And finally, the seven chapters on hydroheritage explore the link between the river flows and the cultural landscape of a region. Joy Sen (chapter 17) presents a deep exploration of three principal rivers (Ganga, Yamuna and Sarasvati), which collectively reinforces the deep ecosystem sustaining the northern Indian Plains. A detailed account of water practices in India since ancient ages has been provided by Jain et al(chapter 18). Authors state that extensive use of technology at all scales would become essential to address the increasing water stresses in India. The impact of geodynamics and tectonics on shaping the river migration and water resource availability in many parts of thickly populated Indo-Gangetic alluvial plain has been discussed Kaushik et al (chapter 19) with a special reference to Vedic River Saraswati. Similar studies were presented for riverine systems in Odisha region by Jana et al (chapter 21) and Bengal region by Kalyan Rudra (chapter 22).

Our research group (Isotope and Radiation Application Division, BARC) presented the impact of river flow on groundwater recharge (chapter 20). Here we explained the dynamics of the groundwater recharge and interconnectivity between various zones using environmental stable and radioisotopes. We propose that the major control on the groundwater dynamics is hydrogeological anisotropy of the subsurface and also highlight that deep groundwater sustainability is questionable due to presence of paleo-waters in this region.This chapter also highlights the need for augmenting the shallow aquifer recharge through rainwater conservation, failing which might adversely impact the future water security in this region. In my view, this book is the first step towards integration of ideas, history and knowledge of this invaluable resource for this immensely populous and diplomatically important area of the world, such that we would be able to effectively understand, manage and preserve the rivers for our future generations.

*Author for Correspondence: Dr. Tirumalesh Keesari
E-mail: tirumal@barc.gov.in

in short about the book

- **A unique knowledge on**
  the river studies for historians, scientists, planners, social scientists and policymakers, and are written by leading experts and researchers from across the globe
- **Provides a practical understanding of**
  the inherent issues of river ecology, their conservations, chronicles and governance through multi-faceted state-of-art knowledge of hydrology, hydrosocial and hydro-heritage approaches

Reports from symposia, workshops and conferences

Dr. R. Chidambaram, Former Chairman AEC, speaking at 2023 edition of SSPS held at BIT (Mesra).

The 2022 edition of 66th DAE Solid State Physics Symposium was organized at the Birla Institute of Technology situated at Mesra in Ranchi, Jharkhand during December 18-22. The symposium was sponsored by BRNS and the scientific program was planned and organized by Physics Group, BARC.

From the 800 contributory papers received for the symposium, 711 were chosen for final presentation. Besides, 3 plenary talks, 39 invited talks, 32 oral presentations, and 578 posters were part of the symposium.

The three talks delivered in the plenary segment are “Metavalent Bonding Origins of Unusual Properties of Group IV Chalcogenides” by Prof. Umesh V. Waghmare, JNCASR, Bangalore; “Premartensitic and Precursor Phenomena in Magnetic Shape Memory Alloys” by Prof. Dhananjai Pandey, IIT, BHU, Varanasi and “Light matter interactions in 2D semiconductors for quantum photonics” by Prof. Samit K. Ra, IIT, Kharagpur.

Dr. R. Chidambaram, Former Chairman, AEC, delivered his talk titled “From Raman Effect to Nuclear Power”. Prof. Indranil Manna, Vice Chancellor, BIT (Mesra) gave his talk on the topic “Science–Engineering–Technology Synergy Needed for Technological Self Reliance”. A talk on “Quantum Magnetism in Spin Systems of Lower Dimension” was delivered by Dr. S. M. Yusuf, Director, Physics Group, BARC.

2 Young achievers, 3 best Ph.D. theses and 29 best posters have been recognized and were duly awarded at the event. The proceedings of the event were uploaded online in DAE SSPS website (www.daessps.in)

Symposium topics

- Phase transitions
- Soft Matter, including Polymer & Biological Systems
- Nano-materials
- Experimental Techniques and Devices
- Single Crystal, Glasses and Amorphous Systems
- Surfaces, Interfaces and Thin Films
- Electronic Structures and Phonons
- Dielectric, Ferroelectric and Piezoelectric
- Transport Properties
- Semiconductor and Spintronics
- Magnetism and Superconductivity
- Energy Materials
- 1-D, 2-D and quantum Materials

Reports from symposia, workshops and conferences

NSRP-2023
Radiation and Photochemistry Symposium

Proceedings of NSRP-2023 released during the Inaugural Function.
(L-R) Dr. Atanu Barik (RPCD, BARC), Dr. Nandita Maiti (RPCD, BARC), Dr. A. K. Tyagi (Chemistry Group, BARC), Dr. Awadhesh Kumar (RPCD, BARC), Prof. Meenal Kowshik (Associate Dean SRCD, BITS Pilani, Goa) and Prof. Mainak Banerjee, (Department of Chemistry, BITS Pilani, Goa).

The 15th National Symposium on Radiation and Photochemistry (NSRP-2023) was held at BITS Pilani, K. K. Birla Goa campus during January 05-07, 2023. The Radiation & Photochemistry Division (RPCD) of Chemistry Group, BARC along with Indian Society for Radiation and Photochemical Sciences (ISRAPS) and Department of Chemistry, BITS Pilani, Goa organized the symposium, which included 9 scientific sessions, comprising 20 invited lectures by eminent scientists across India, and 121 contributory paper presentations. 150 delegates, including 20 eminent scientists from BARC and other reputed Indian R&D institutes attended the three-day scientific program.

The proceedings of the symposium have been covered in detail in a souvenir, which was released by Dr. A. K. Tyagi, Director, Chemistry Group, BARC during the inaugural function. A special ISRAPS bulletin was also unveiled at the program. The fundamental aspects of Radiation & Photochemical sciences, Applications of radiation & photochemistry, Theoretical aspects of radiation & photochemistry, Radiation & photochemistry of advanced materials, Atmospheric chemistry and Radiation & photochemistry in nuclear industry and healthcare and biology/life sciences have been covered in the form of lectures and presentations by the participants. Some important applications in the areas of current interest, such as energy, environment and health, were discussed.

Meritorious young researchers have been recognized by awarding them with Dr. Harimohan Memorial Award in Radiation Chemistry and Dr. P.K. Bhattacharya Award in Photochemistry during the symposium. NSRP-2023 was partially funded by the Board of Research in Nuclear Sciences (BRNS), and Science and Engineering Research Board (SERB), India.

Symposium topics

- **Basic studies in radiation & photochemical sciences**
- **Applications of radiation & photochemistry**
- **Theoretical aspects of radiation & photochemistry**
- **Radiation & photochemistry of advanced materials**
- **Atmospheric chemistry**
- **Radiation & photochemistry in nuclear industry, health care and biology/life sciences**

Reports from symposia, workshops and conferences

The release of proceedings of BEAM-22. Left to Right: Dr. Anil Boda, ChED, Dr. Sk. Musharaf Ali, Head AMCAS, ChED, Prof. B.K. Dutta, Institute Chair Professor (HBNI), Dr. K.T. Shenoy, Director, ChEG, Dr. Pooja Sahu, ChED and Rupsha Bhattacharyya, HWD, BARC.

BEAM-22

Theme Meeting on 'Bridging Experiments and Atomistic Modeling'

A one-day theme meeting "Bridging Experiments and Atomistic Modeling" (BEAM-22) was organized at Training School Hostel BARC, Mumbai on November, 4, 2022 by Chemical Engineering Division, BARC in collaboration with the Board of Research in Nuclear Sciences (BRNS), Department of Atomic Energy (DAE).

Shri K.T. Shenoy, Director, Chemical Engineering Group and Chairman, BEAM-22 started the proceedings of the meeting with his welcome address. Dr. B. K. Dutta, Institute Chair Professor, HBNI and Chief Guest of the meeting, in his inaugural speech advocated the needs of multi-scale modeling approach for deciphering complex real problems. He also emphasized on increased cohesiveness between theory, computation and experimentation in various branches of science and engineering for careful conceptualization and successful implementation of research problems. He also advocated the need for constituting an ideal forum, which can function as a bridge for understanding theoretical aspects of atomistic modeling and experiments. The proceedings of the theme meet was unveiled by the Chief Guest. The vote of thanks was delivered by Dr. Sk. Musharaf Ali, Head, AMCAS, ChED and Convener, BEAM-22. Close to 100 delegates from DAE and non-DAE institutes participated in the meeting.

Total 15 invited lectures were delivered on various aspects of atomistic modeling, including application of computational tools for selection of suitable adsorbents for the extraction of metal ion and isotope separation, design of new molecules using machine learning, selection of glass composition for nuclear waste immobilization, thermodynamics of nuclear materials, tailor made deep eutectic solvents, and materials for alternative energy. Experts from various institutes, including IISc, TIFR, IACS (Kolkata), HRI (Prayagraj), IIT (Mumbai, Chennai, Guwahati) and BARC made presentations on various aspects of the theme meeting. In the concluding session, a panel discussion was conducted in which Shri K.T. Shenoy, Director, Chemical Engineering Group stressed the provision of a suitable platform, which can be leveraged properly by groups involved in atomistic and continuum modeling as well as experimentalists for solving complex chemical processes pursued by the Department of Atomic Energy. The registration of a new "Society for Atomistic and Continuum Modeling (SACM)" to bring all stakeholders of atomistic modeling and continuum modeling under a common roof was announced by Dr. Sk. Musharaf Ali (Convenor, BEAM-22). The proposed society would function under the auspices of Chemical Engineering Division, BARC, Trombay.

Reports from symposia, workshops and conferences

Dr. R.B. Grover, Member, Atomic Energy Commission, addressing a gathering of audience present at the Theme Meeting on Hydrogen Energy and Technology (HET-2023).

Theme Meeting on Hydrogen Energy and Technology

The Apex Committee on "Hydrogen Energy Program", BARC organized a 2-day National Theme Meeting on Hydrogen Energy and Technology 2023 on 23 and 24th January 2023 at the DAE Convention Centre, Anushaktinagar, Mumbai. About 160 participants from DAE units and various public and private industrial organizations participated in this event. The objectives of this event were three-fold:

To showcase the hydrogen energy and economy related research and development activities and commercialization initiatives being carried out at BARC and other research organizations.

To obtain firsthand accounts of the industrial organizations' interest, current plans and programs towards deployment of hydrogen production and utilization technologies.

To identify possible collaborative activities between BARC and industrial sectors that may be taken up to advance the National Hydrogen Energy Program, announced on January 4, 2023.

Thematic areas discussed

- Hydrogen Generation
- Hydrogen Storage and Storage Devices
- Hydrogen Utilization and Safety

There were 21 presentations made in course of the two days, covering hydrogen production, storage and utilization, other than the key note session. The final day saw a panel discussion to summarize the proceedings of the meeting and to seek directions for the way ahead.

Based on the presentations and panel discussion held during the meeting, the following points may be considered regarding the way forward:

- Collaborative activities leveraging the individual strengths of the different collaborators are required. The multiple joint undertakings and projects between the PSUs and academic institutions show that this is the preferred pathway to accelerate system development and deployment.
- The pursuit of a technology development program should be prioritized on the basis of users of that technology. The technology transfer and scale up programs of BARC's alkaline water electrolyser technology reflects this approach. A systematic approach to generating and protecting intellectual property rights is also necessary in this regard.
- Commercial aspects must be taken into account from the initial stages of development; scientists must develop an appreciation of project economics to guide technology development work.

Reports from symposia, workshops and conferences

Release of Souvenir on AOCRP-6 during the inaugural day.

Asian and Oceanic Congress for Radiation Protection

The Indian Association for Radiation Protection (IARP) and the Asian and Oceanic Association for Radiation Protection (AOARP) jointly organized the sixth edition of Asian and Oceanic Congress for Radiation Protection (AOCRP6) with the theme *Radiation Protection and Surveillance in Nuclear, Medical, Industrial Facilities and the Environment* during February 7-11, 2023 at Nehru Centre, Worli, Mumbai.

The scientific deliberations of the conference included latest developments in radiological surveillance at nuclear facilities and environment, assessment of radiation exposure to the public from natural radiation, environmental radioactivity, radiation dosimetry and preparedness to potential emergencies. The conference deliberations included 32 invited talks, 2 oratory talks, 92 oral presentations, 365 poster presentations and a panel discussion on *Radiation protection of people and the Environment: Future Perspectives.*

The conference was attended by about 450 delegates, including Radiation Protection professionals from India and abroad (particularly from Asian and Oceanic countries), DAE establishments, experts from ICRP, IAEA, IRPA and Japan Health Physics Society, students from educational institutions from India and abroad, and Radiation Safety Officers (RSO) of hospitals and industry.

A dedicated special session of IRPA young generation network (IRPA-YGN) forum was conducted on February 11 to generate a network among young radiation protection professionals in Asia Oceanic region on various issues related to career in radiation protection and safety in nuclear energy program, scientific developments in this field, public awareness.

One of the important outcomes of the AOCRP6 congress was that “ICRP has considered deliberating on the revision of dose limits for the workers and public based on the scientific contents and discussions held during AOCRP6, in their future reviews on Revision of System of Radiation Protection”.

Reports from symposia, workshops and conferences

Release of Souvenir on NSD2023 during the inaugural day.

NSD2023 on New Generation Nuclear Reactors

The National Science Day is celebrated every year on 28th February to commemorate the discovery of *Raman Effect* by renowned Indian Scientist and Nobel Laureate Prof. C. V. Raman. The aim of this celebration is to provide a platform for fruitful interactions between the students from various schools/colleges and leading scientists of BARC, as well as to emphasize on the significant role of science for the benefit of the society.

This year, it was celebrated at Central Complex Auditorium during 28th February to 2nd March 2023, with the theme *New Generation Nuclear Reactors*, to spread awareness about Nuclear Power as a clean, safe and sustainable option for our ever-increasing energy demands and global wellbeing.

More than 650 students and teachers from around 30 schools/colleges from Mumbai and Navi Mumbai have visited BARC Trombay. Audio-visuals, skits, quizzes, invited talks by eminent personalities on the topics broadly related to the theme, visits to various laboratories, exhibition of working models etc. were also organized. All these programs were planned to popularize scientific thinking, as well as to open up the new frontiers to the young minds.

Participants from various colleges and schools in Mumbai.

Reports from symposia, workshops and conferences

Participants of the training course in Isotope Hydrology conducted at CGWB.

Training Course on Isotope Hydrology

Bhabha Atomic Research Centre, Trombay and the Ministry of Jal Shakti (Water Resources) have joined hands to collaborate in an exercise for training and equipping the officials of Central Ground Water Board (CGWB) in the field of Isotope Hydrology. The training program was organized in two stages – classroom lectures at a dedicated facility of CGWB followed by practical training in BARC Trombay campus.

In the first leg of the program, a classroom based training course comprising lectures as well as case studies on Isotope techniques and its application in groundwater, was conducted at the Rajiv Gandhi National Ground Water Training & Research Institute (RGNGWTRI) in Raipur during November 7-11, 2022, by senior officers of Isotope and Radiation Application Division (IRAD), Bhabha Atomic Research Centre.

This was followed by a four-day training program (December 19-23) in BARC Trombay during which senior officers of BARC offered practical training in isotope hydrology techniques to CGWB officials. The specialized areas covered in this program include demonstration of sampling protocols to be followed for the measurement of various isotopes (both stable & radioactive) in water, training on the operation of various laboratory instruments such as Isotope Ratio Mass Spectrometer (IRMS), Low Level Liquid Scintillation Counter (LSC), Alpha Spectrometer, Radon monitor, Radium Delayed Coincidence Counter (RaDeCC), NaI Scintillation detectors, Ion Chromatograph (IC), field equipment.

Dr. J. Noble of BARC acted as the coordinator for the training program. Technical lectures on various topics in isotope hydrology were delivered by Dr. H.J. Pant, Dr. U.K. Sinha, Dr. J. Noble, Dr. K. Tirumalesh and Dr. S. Chatterjee of BARC.

Participants of the 43rd course on 'Safety and Regulatory Measures for BARC Facilities' conducted at DAE Convention Centre, Anushaktinagar, during June 22-25, 2022.

Training Program
on safety and regulatory measures

The BARC Safety Council Secretariat (BSCS) conducts short term training courses for scientific and technical personnel of BARC facilities regularly. The 43rd course on 'Safety and Regulatory Measures for BARC Facilities' was conducted during June 22-25, 2022, which saw participation of sixty-one individuals from BARC.

Important topics addressed in the course include regulatory framework of BARC, radiation basics and natural radiation, radiological safety in front-end and back-end nuclear facilities, electrical safety, occupational health care, biological effects of radiation, industrial hygiene and safety, safety in storage and handling of chemicals, industrial safety aspects in fuel fabrication facilities, safety aspects of material handling equipment, regulatory aspects of radioactive waste management, regulatory inspections, event reporting, emergency preparedness and response to nuclear & radiological emergencies, and improvement of safety culture in the facilities.

Indian Science Congress '23

glimpses

ISCA Young Scientist Award to BARC scientist

Mr. Rajath Alexander is currently working as Scientific Officer/D in Glass and Advanced Materials Division, Bhabha Atomic Research Centre (BARC), Mumbai. He graduated from the 14th batch (DGFS) of BARC Training School in 2017 in the discipline of Metallurgical Engineering. He completed his M. Tech in Metallurgical Engineering from IIT Madras in 2017, where he received Dr. M.N. Dhandapani Prize and Sudharshan Bhat Memorial Prize for exceptional academic performance in M. Tech. Mr. Alexander specializes in synthesis and technology development for carbon nanomaterials by floating catalyst chemical vapour deposition and manufacturing of composites using nano reinforcement. He received the DAE Group Achievement Award in 2019 in recognition of his efforts which helped in supply of bullet-proof jackets ('Bhabha Kavach') to meet the requirements of CISF. Mr. Alexander has published around 16 articles in peer-reviewed international journals. He also presented papers in several international conferences. Recently, Mr. Alexander has been awarded the prestigious Indian Science Congress Association Young Scientist Award 2023 for his work on synthesis of three-dimensional self-assembled carbon nanotube aerogel and its application as a high performance virus filter in the domain of Material Science. The Indian Science Congress Association Award recognizes outstanding work in different fields of science and engineering, and is presented to researchers below the age of 32.

Sir C. V. Raman and Dr. Vikram Sarabhai

Edited & Published by
Scientific Information Resource Division
Bhabha Atomic Research Centre, Trombay, Mumbai-400 085, India
BARC Newsletter is also available at URL:https://www.barc.gov.in